

ABSTRACT

FINITE ELEMENT ANALYSIS OF A TRIANGULAR
BEAM SEAT STIFFENER PLATE

by

Phillip Anthony Krupa

Master of Science in Civil Engineering

Youngstown State University, 1978

Submitted in Partial Fulfillment of the Requirements

for the Degree of

Master of Science in Engineering


in the

Civil Engineering

Program


Adviser

2/9/78
Date


Dean of the Graduate School

2/15/78
Date

YOUNGSTOWN STATE UNIVERSITY

January, 1978

ABSTRACT

FINITE ELEMENT ANALYSIS OF A TRIANGULAR
BEAM SEAT STIFFENER PLATE

Phillip Anthony Krupa

Master of Science in Civil Engineering

Youngstown State University, 1978

Beam seat stiffeners, such as those employed for beam and crane girder connections in industrial building, are structural elements which, to date, are designed using rule-of-thumb procedures. Both theoretical and experimental results of previous investigations into this problem are available. The proposed design methods contained therein, however, are encumbered with complex equations and multiple graph value determinations. For these reasons, current design practice usually involves providing stiffener plate thicknesses considerably in excess of that of the supported member's web, rather than making any realistic attempt to optimize the design with a minimum thickness.

The finite element method of analysis was used in this study to determine the stress levels within a triangular stiffener plate. These findings were combined with earlier theoretical and experimental investigations to rationally develop design aids which will enable a designer to quickly determine a minimum stiffener plate thickness. Both yield stress limitations and buckling considerations were incorporated into the design aid formulations.

ACKNOWLEDGEMENTS

The author wishes to express his gratitude to his adviser, Dr. Jack D. Bakos, Jr., for his time, support, encouragement, and advice which he provided in the development, preparation, and completion of this thesis.

The author also wishes to thank Dr. Gus Mavrigan and Dr. Paul X. Bellini for their time and valuable suggestions in the development of this work.

Finally, a special appreciation is held for Miss Kimberly Smidt, who typed this manuscript, and for Miss Mary Ann Hammond, who proofread this manuscript.

1.2 Classical Approaches to Buckling Problem.....	3
1.3 Salmon's Approaches to the Buckling Problem.....	4
1.4 Experimental Verification of Salmon's Findings.....	5
1.5 Summary of Existing Design Techniques...	10
II. DETERMINING THE FINITE ELEMENT MODEL AND PRELIMINARY TESTING FOR ACCURACY.....	14
2.1 Selection of Finite Element Computer Program.....	14
2.2 The Finite Element Model.....	14
2.2.1 The Element Configuration and Boundary Conditions.....	15
2.2.2 Load Distribution.....	16
2.2.4 Preliminary Testing to Determine the Extent of Stress Variation Due to A Variation in the Load Distribution.....	17
2.2.5 Final Selection of Model Configuration.....	20

TABLE OF CONTENTS

	PAGE
ABSTRACT.....	ii
ACKNOWLEDGEMENTS.....	iii
TABLE OF CONTENTS.....	iv
LIST OF SYMBOLS.....	vi
LIST OF FIGURES.....	viii
LIST OF TABLES.....	x
CHAPTER	
I. INTRODUCTION.....	1
1.1 Problem Statement.....	1
1.2 Classical Approaches to Buckling Problem.....	3
1.3 Salmon's Approaches to the Buckling Problem.....	4
1.4 Experimental Verification of Salmon's Findings.....	5
1.5 Summary of Existing Design Techniques...	10
II. DETERMINING THE FINITE ELEMENT MODEL AND PRELIMINARY TESTING FOR ACCURACY.....	14
2.1 Selection of Finite Element Computer Program.....	14
2.2 The Finite Element Model.....	14
2.2.1 The Element Configuration and Boundary Conditions.....	15
2.2.3 Load Distribution.....	16
2.2.4 Preliminary Testing to Determine the Extent of Stress Variation Due to A Variation in the Load Distribution.....	17
2.2.5 Final Selection of Model Configuration.....	20

TABLE OF CONTENTS (CONT.)

SYMBOL	DEFINITION	UNITS	PAGE
x	Local Horizontal Coordinate	inches	
	2.3 Scope of Analysis Program.....		24
III.	PRESENTATION OF RESULTS.....		29
	3.1 Final Analysis.....		29
	3.2 Results.....		29
	3.3 Design Examples.....		52
	3.4 Mathematical Formulations.....		55
	3.5 Design Recommendations.....		58
IV.	CONCLUSIONS.....		60
APPENDIX A.		62
LIST OF REFERENCES CITED.		89
t	Plate Thickness	inches	8
A/B	Aspect Ratio	none	8
R	Resultant Load	Kips	9
F _y	Yield Stress	KSI	12
T _{web}	Supported Beam Web Thickness	inches	12
α	Interior Angle Between Free Edge and Supported Edge	degrees	12
R'	Resultant Column Load	Kips	12
b	Point of Intersection of Loaded and Supported Edges	none	13
b'	Midpoint of Free Edge	none	13
e	Load Eccentricity	inches	13
	Poisson's Ratio	none	17
E	Young's Modulus	psi, KSI	17

LIST OF SYMBOLS			
SYMBOL	DEFINITION	UNITS	PAGE
x	Local Horizontal Coordinate	inches	1
y	Local Vertical Coordinate	inches	1
A	Loaded Edge Length	inches	1
B	Supported Edge Length	inches	1
Z-C	Zienkiewicz-Cheung	none	2
cr	Critical Buckling Stress	KSI	4
V	Critical Edge Displacements	inches	4
u	Local Horizontal Coordinate	inches	4
v	Local Vertical Coordinate	inches	4
w	Local Out-of-plane Coordinate	inches	4
K	Stiffness Coefficient	10^8 psi	4
t	Plate Thickness	inches	4
A/B	Aspect Ratio	none	8
R	Resultant Load	Kips	9
F _y	Yield Stress	KSI	12
T _{web}	Supported Beam Web Thickness	inches	12
α	Interior Angle Between Free Edge and Supported Edge	degrees	12
R'	Resultant Column Load	Kips	12
b	Point of Intersection of Loaded and Supported Edges	none	13
b'	Midpoint of Free Edge	none	13
e	Load Eccentricity	inches	13
	Poisson's Ratio	none	17
E	Young's Modulus	psi, KSI	17

SYMBOLS	DEFINITION	UNITS	PAGE
Δ_{max}	Maximum Stress Position	none	23
D/C	Free Edge Stress Location	none	25
q	Assumed Load Distribution	Kips/Foot	26
L	Free Edge Length	inches	34
[K]	Stiffness Matrix	Kips/inch	37
Area	Element Area	inches ²	37
{ σ }	Stress Matrix	Kips/inch ²	37
[D]	Elasticity Matrix	Kips/inch ²	37 ⁰
{Q}	Load Matrix	Kips	37
{B}	Displacement Matrix	inches	37
D	Constant Coefficient	Kips/inch	57

LIST OF FIGURES

FIGURE	PAGE
1.1 Welded Construstion.....	1
1.2 Critical Buckling Displacement.....	5
1.3 Theoretical Design Curve.....	6
1.4 Theoretical Buckling Stresses.....	7
1.5 The Experimental Study's Load Application.....	9
1.6 Adjusted Stiffness Curve.....	11
1.7 Current Buckling Consideration.....	13
2.1 Possible Configurations.....	15
2.2 Boundary Conditions.....	16
2.3 Load Distribution Cases.....	18
2.4 Load Case Stress Variance.....	22
2.5 Free Edge Stress Location.....	26
2.6 The F.E. Model and Element Numbering.....	27
3.1 Longitudinal Free Edge Stress Distribution....	30
3.2 Longitudinal Free Edge Stress Distribution....	31
3.3 Longitudinal Free Edge Stress Distribution....	32
3.4 Longitudinal Free Edge Stress Distribution....	33
3.5 Maximum Longitudinal Stress Directions.....	34
3.6 Load Case 3 Stresses.....	36
3.7 Triangular Plane Stress Element.....	37
3.8 Thickness Based Upon Yield Criteria.....	40
3.9 Critical Buckling Thicknesses.....	42
3.10 Design Chart: Combined Criteria.....	44
3.11 Design Chart: Combined Criteria.....	45

LIST OF FIGURES (CONT.)

FIGURE	PAGE
3.12 Design Chart: Combined Criteria.....	46
3.13 Design Chart: Combined Criteria.....	47
3.14 Design Chart: Combined Criteria.....	48
3.15 Design Chart: Combined Criteria.....	49
3.16 Design Chart: Combined Criteria.....	50
3.17 Design Chart: Combined Criteria.....	51
3.18 Stress-Aspect Ratio Relationship.....	56
3.19 Applicable Construction.....	58
A.1 Sample Problem.....	81

LIST OF TABLES

TABLE	PAGE
1.1 Experimental Study Plate Schedule.....	8
2.1 Preliminary Testing Program.....	19
2.2 Maximum Free Edge Stress as a Ratio of D/C....	25
2.3 Comparison of Maximum Stress Results.....	23
2.4 Plate Testing Schedule.....	28
3.1 Design Specification Comparison Thickness and and Failure Mode.....	53
3.2 Comparative Design Study.....	54



Fig. 1.1. Welded Construction

The analysis of the welded assembly was accomplished using the finite element technique⁽¹⁾ along with the Zienkiewicz-Cheng⁽²⁾ finite element program. The results from the analysis were combined and compared with previous theoretical⁽³⁾ and experimental⁽⁴⁾ investigations in order to develop a usable design aid.

*Number in parenthesis indicates reference cited.

CHAPTER I

INTRODUCTION

1.1 Problem Statement

The objective of this study was to investigate the elastic behaviour of triangular stiffener plates, which are frequently employed for beam/column connections. Fig. 1.1 shows a typical application of a triangular stiffener plate in welded construction.

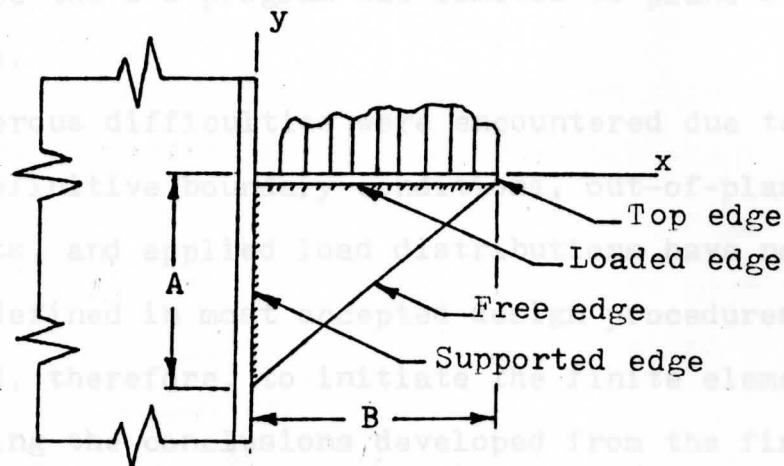


Fig. 1.1. Welded Construction

The analysis of the welded assembly was accomplished using the finite element technique^{(1)*} along with the Zienkiewicz-Cheung⁽²⁾ finite element program. The results from the analysis were combined and compared with previous theoretical⁽³⁾ and experimental⁽⁴⁾ investigations in order to develop useable design aids.

*Number in parenthesis indicates reference cited.

When a designer is confronted with specifying the proportions of a triangular stiffener plate, two distinct, yet related, constraints present themselves. These are:

- 1.) The location and magnitude of the maximum stress (Δ_y).
- 2.) The location and magnitude of the critical buckling stress (Δ_{CR}).

A finite element analysis could provide the location and magnitude of the maximum plane stress and the maximum free edge stress. However, it was necessary to employ mathematical formulations⁽³⁾ in the determination of the critical buckling stress, since the Z-C program was limited to plane stress applications.

Numerous difficulties were encountered due to the fact that definitive boundary conditions, out-of-plane displacements, and applied load distributions have not been completely defined in most accepted design procedures. It was required, therefore, to initiate the finite element analysis using the conclusions developed from the findings of the theoretical work by Salmon⁽³⁾ and the experimental work by Buettner & O'Sheridan⁽⁴⁾.

The following statements form a basis for the finite element approach to this problem: (See Figure 1.1)

- 1.) Translations in the x and y directions of the supported vertical edge were zero.
- 2.) Translation in the x direction of the loaded edge was prevented.
- 3.) Loading conditions were varied.
- 4.) Displacements were entirely in plane.

- 5.) Rotations of the triangular plate due to column bending were ignored.
- 6.) The plate remained an in-plane entity until buckling occurred.

Before the finite element analysis approach can be presented, pertinent previous theoretical and experimental work will be reviewed, in detail, where necessary.

1.2 Classical Approaches to Buckling Problem

Timoshenko⁽⁵⁾ first attempted to solve the buckling problem by finding the solution of the differential equation, which described the problem in terms of stress distribution. However, since the stress distribution is neither constant, nor is there a readily expressible variation throughout the triangular stiffener plate, the resulting differential equation becomes considerably complex. Therefore, even though the differential equations may have led to a solution, the considerable complexities involved eliminated any practical use of the technique.

In other attempts to solve the buckling problem, both Timoshenko⁽⁵⁾ and Ritz⁽⁶⁾ developed equations describing the behaviour of the triangular plate (See Figure 1.1) in terms of equilibrium and potential energy. In order to satisfy all of the boundary conditions, expressions for the displacements must be developed. These expressions proved to be extremely difficult and cumbersome to develop. The energy approach to the problem had to be either discarded or modified if it was to be a practical solution to the buckling problem.

1.3 Salmon's Solution to the Buckling Problem

Salmon⁽³⁾ used the generalized energy methods employed by both Timoshenko⁽⁵⁾ and Ritz⁽⁶⁾ for the solution to the buckling problem (See Figure 1.2). Salmon took advantage of a unique feature of the energy approach, i.e., expressions for displacements need not satisfy all boundary conditions, but only these geometric requirements along the edges of the triangular plates. Expressions for displacements in the conventional u , v , and w directions were established by Salmon using a power series form for both simply supported and fixed supported plates (These support conditions apply to the supported edge shown in Figure 1.1).

The solution to the power series equations yielded the critical value V_0 (See Figure 1.2) at which buckling was imminent. With this value known, the stress distributions were then determined along the edges of the triangular plate. The maximum stresses when buckling was imminent were the free edge stresses and thus, the critical buckling stresses magnitude and locations were determined. These values depend upon the support conditions of the plate, either simply supported or fixed along the supported edge.

Salmon then developed a relationship which expressed the critical stress for both fixed and simply supported edge conditions. The equation takes the form

$$\sigma_{CR} = \frac{K}{(A/t)^2} \quad (1.1)$$

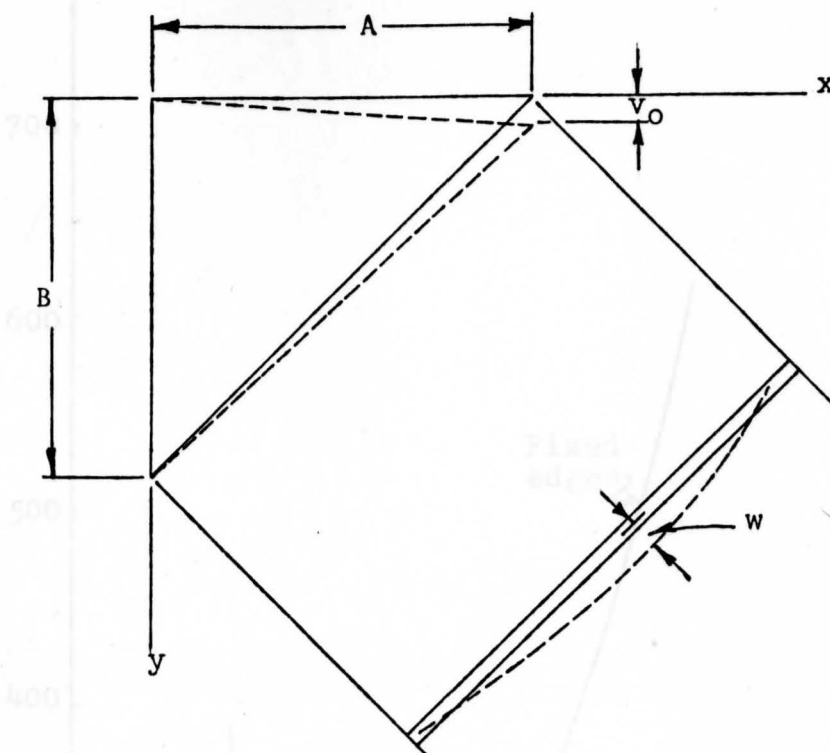


Fig. 1.2. Critical Buckling Displacement

The buckling coefficient K , which is a function of the material properties, has a single value for all plates having the same aspect ratio (loaded to supported edge ratio) and the same supported edge conditions. Figure 1.3 shows the variation of K with respect to the aspect ratio and the supported edge condition. These variations grouped graphically, show the critical buckling stresses for different sizes and thickness of plates (See Figure 1.4).

1.4 Experimental Verification of Salmon's Findings

Physical testing of triangular stiffener plates was performed by Buettner and O'Sheridan⁽⁴⁾ as a follow-up of

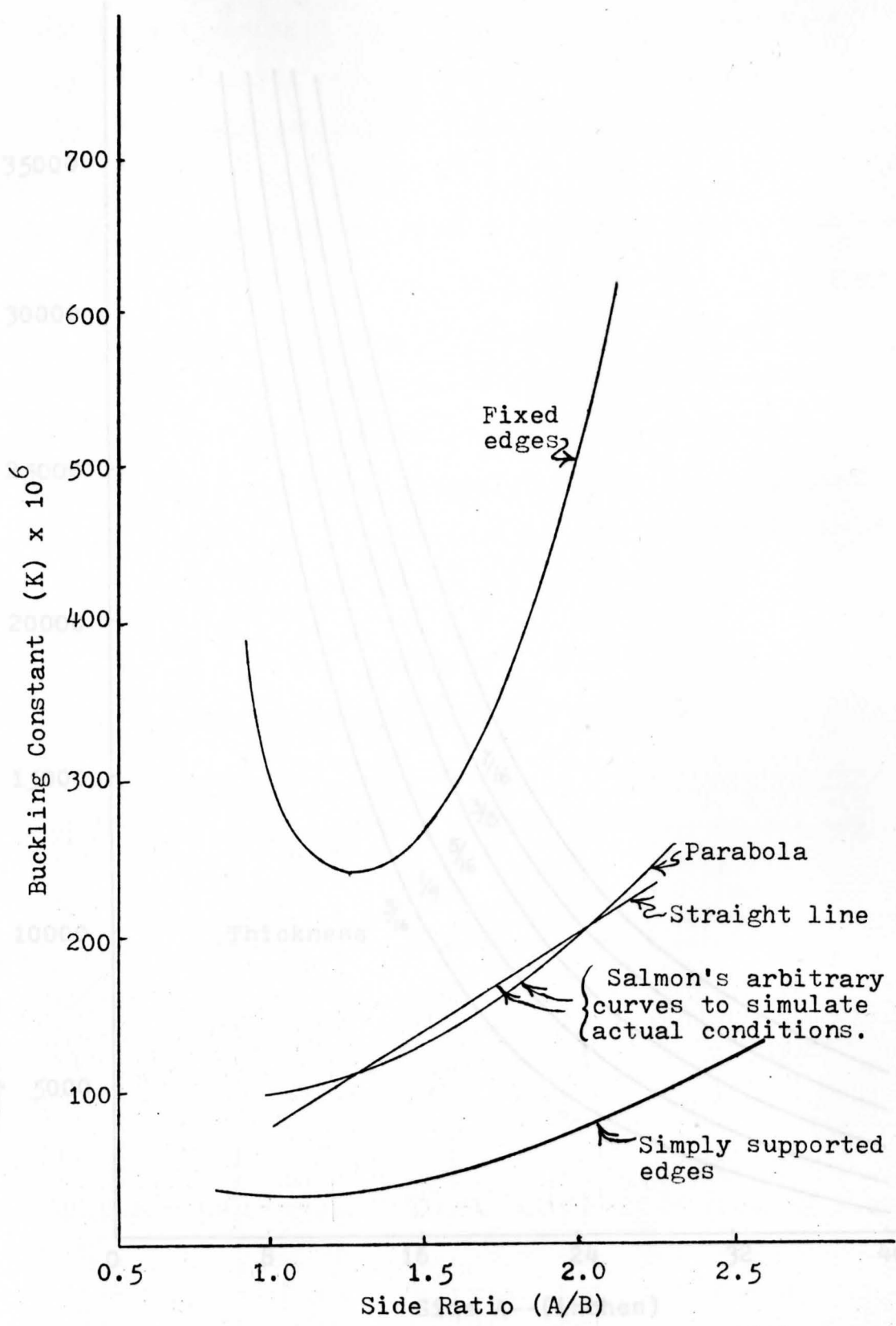


Fig. 1.3. Theoretical Design Curve⁽³⁾

Fig. 1.4. Theoretical Buckling Stresses⁽³⁾

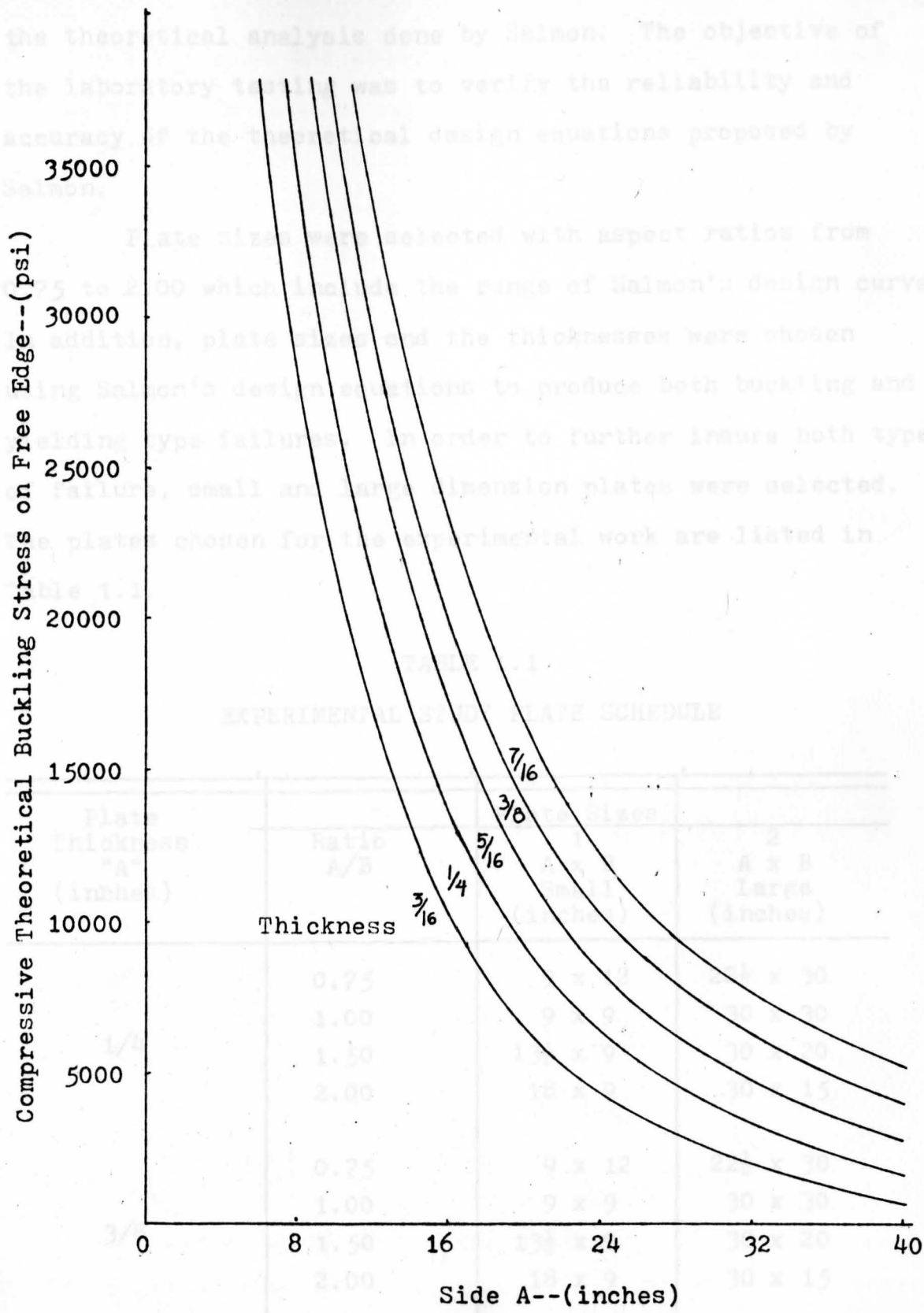


Fig. 1.4. Theoretical Buckling Stresses⁽³⁾

the theoretical analysis done by Salmon. The objective of the laboratory testing was to verify the reliability and accuracy of the theoretical design equations proposed by Salmon.

Plate sizes were selected with aspect ratios from 0.75 to 2.00 which include the range of Salmon's design curves. In addition, plate sizes and the thicknesses were chosen using Salmon's design equations to produce both buckling and yielding type failures. In order to further insure both types of failure, small and large dimension plates were selected. The plates chosen for the experimental work are listed in Table 1.1.

TABLE 1.1
EXPERIMENTAL STUDY PLATE SCHEDULE

Plate Thickness "A" (inches)	Ratio A/B	Plate Sizes	
		1 A x B Small (inches)	2 A x B Large (inches)
1/4	0.75	9 x 12	22½ x 30
	1.00	9 x 9	30 x 30
	1.50	13½ x 9	30 x 20
	2.00	18 x 9	30 x 15
3/8	0.75	9 x 12	22½ x 30
	1.00	9 x 9	30 x 30
	1.50	13½ x 9	30 x 20
	2.00	18 x 9	30 x 15

The plates and their boundary conditions were designed to duplicate the conditions in Salmon's theoretical study. The load application, which was an important factor in the testing program, was in all cases concentrated along the loaded edge approximately 60% of the distance from the supported edge rather than distributed as is the actual case (See Figure 1.5).

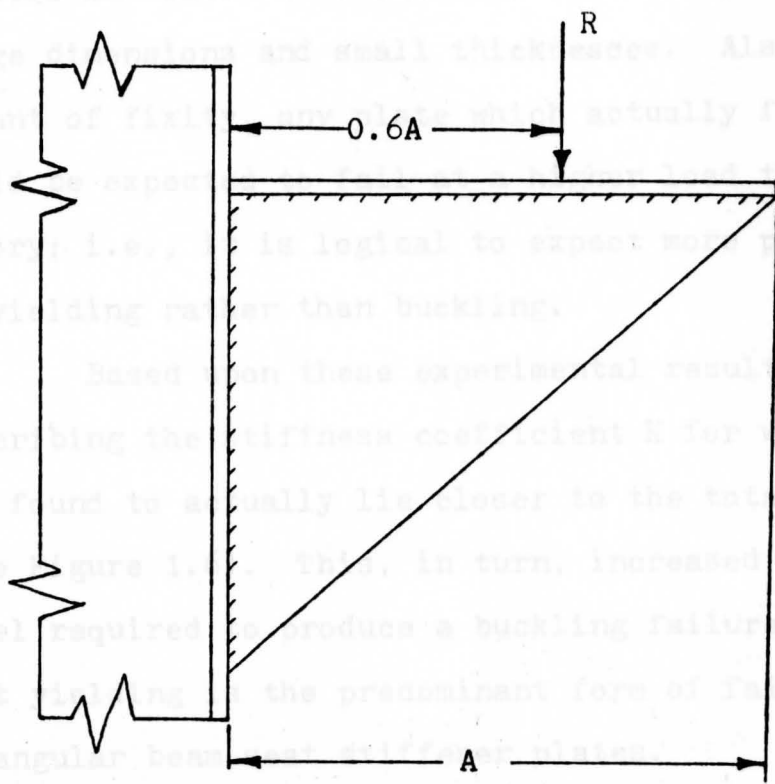


Fig. 1.5. The Experimental Study's Load Application

In order to determine the stress levels and displacements during testing, both SR-4 resistance type and dial type strain gauges were employed. The SR-4 gauges were located at twenty-six positions on each side of the triangular plates,

and the dial gauges in a total of seventeen locations.

Results from the physical testing program differed somewhat from Salmon's theoretical investigation. The 30% fixity along the supported edge as suggested by Salmon (See Figure 1.3) for design purposes was found to be much too conservative. Furthermore, as the aspect ratio became larger, it became nearly impossible to produce a buckling failure in welded construction, even for plates having large dimensions and small thicknesses. Also, with a higher amount of fixity, any plate which actually failed by buckling would be expected to fail at a higher load than predicted by theory; i.e., it is logical to expect more plates to fail by yielding rather than buckling.

Based upon these experimental results, the curve describing the stiffness coefficient K for welded construction, was found to actually lie closer to the totally fixed curve (See Figure 1.6). This, in turn, increased the edge stress level required to produce a buckling failure, and demonstrates that yielding is the predominant form of failure for triangular beam seat stiffener plates.

1.5 Summary of Existing Design Techniques

Current practice allows several different approaches to designing the triangular plates. These are based upon empirical observations and simplifications in load distribution, with the designer usually free to choose whichever system deemed acceptable.

These methods are briefly described as follows: (7)

- 1.) Triangular plate thickness $\geq (T_{WEB})$
- 2.) Triangular plate thickness $\geq (1.4)(T_{WEB})$
- 3.) Triangular plate thickness $\geq \left[\frac{r_{BEAM}}{50} \right] (T_{WEB})$
for $F_y = 50$ KSI
- 4.) Triangular plate thickness $\geq (2)(T_{WEB})$ for A36
- 5.) Triangular plate thickness $\geq (1.5)(T_{WEB})$
for $F_y = 50$ KSI.

Another commonly used approach assumes the plate to act as a cantilever beam (9) in which the results are determined using ordinary beam theory. This results in the employment of excessively thick plates and thus leads to waste of material.

Buckling was not directly considered in either approach since it was assumed that by specifying such large thickness buckling would not occur. However, the possibility of buckling may be conservatively checked by assuming that the reaction (see Figure 1.7) acts

concentrically on the strip which is cross-hatched. This strip forms a column of length AC and rectangular cross-section of $t^*(b \cos \alpha)/4$ which is not arbitrary at all.

It is easily seen that the arbitrary state of design can lead to material waste, particularly if the stiffened web connection is used repeatedly as in pre-engineered buildings applications.

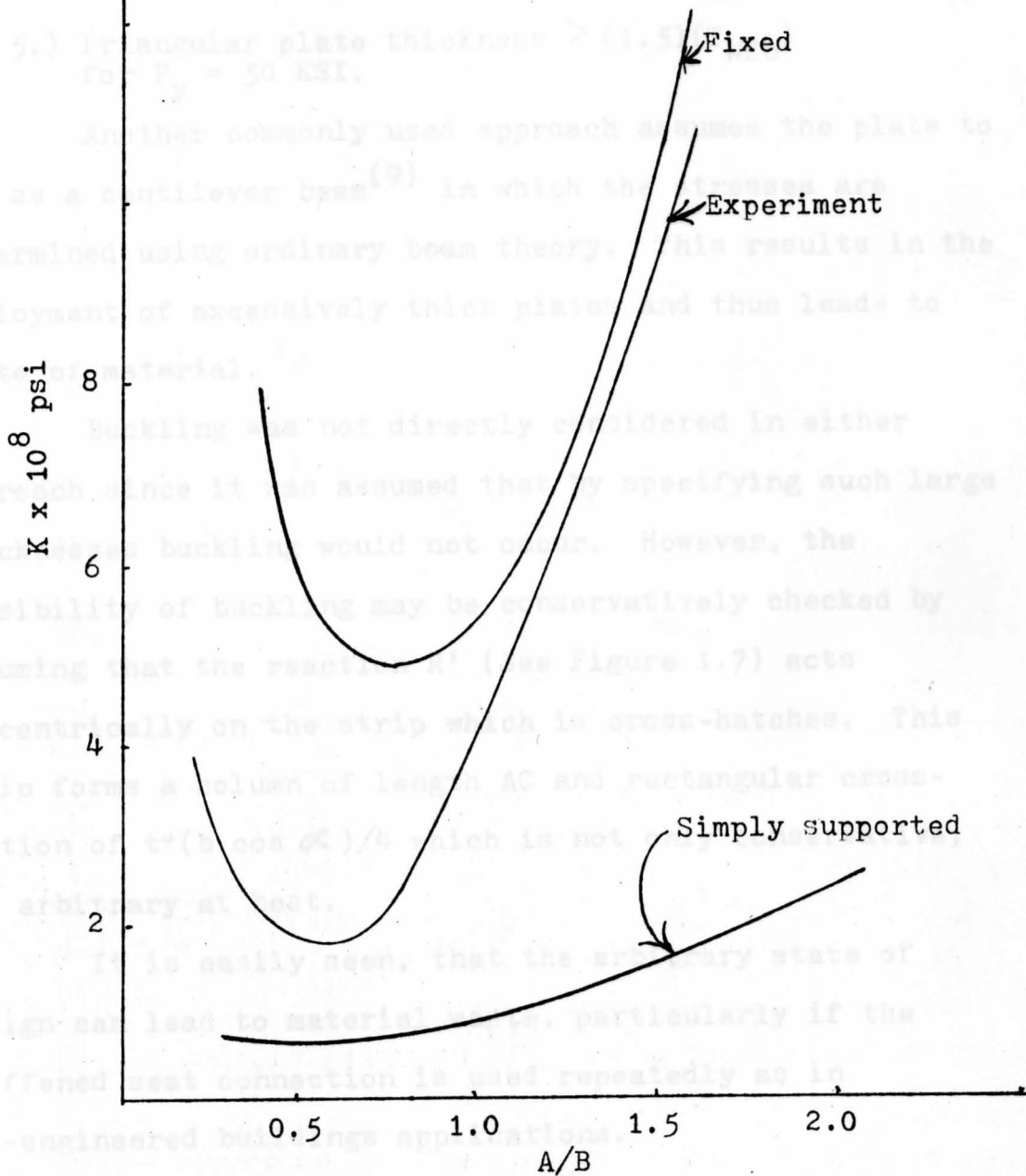


Fig. 1.6. Adjusted Stiffness Curve (4)

These methods are briefly described as follows: (7)

- 1.) Triangular plate thickness $\geq T_{WEB}$
- 2.) Triangular plate thickness $\geq (1.4)(T_{WEB})$
- 3.) Triangular plate thickness $\geq \left(\frac{F_{y_{BEAM}}}{50} \right) (T_{WEB})$
for $F_y = 50$ KSI
- 4.) Triangular plate thickness $> (2)(T_{WEB})$ for A36
- 5.) Triangular plate thickness $> (1.5)(T_{WEB})$
for $F_y = 50$ KSI.

Another commonly used approach assumes the plate to act as a cantilever beam⁽⁹⁾ in which the stresses are determined using ordinary beam theory. This results in the employment of excessively thick plates and thus leads to waste of material.

Buckling was not directly considered in either approach since it was assumed that by specifying such large thicknesses buckling would not occur. However, the possibility of buckling may be conservatively checked by assuming that the reaction R' (See Figure 1.7) acts concentrically on the strip which is cross-hatched. This strip forms a column of length AC and rectangular cross-section of $t*(b \cos \alpha)/4$ which is not only conservative, but arbitrary at best.

It is easily seen, that the arbitrary state of design can lead to material waste, particularly if the stiffened seat connection is used repeatedly as in pre-engineered buildings applications.

CHAPTER TWO

DETERMINING THE FINITE ELEMENT MODEL AND PRELIMINARY TESTING FOR ACCURACY

2.1 Selection of Finite Element Computer Program

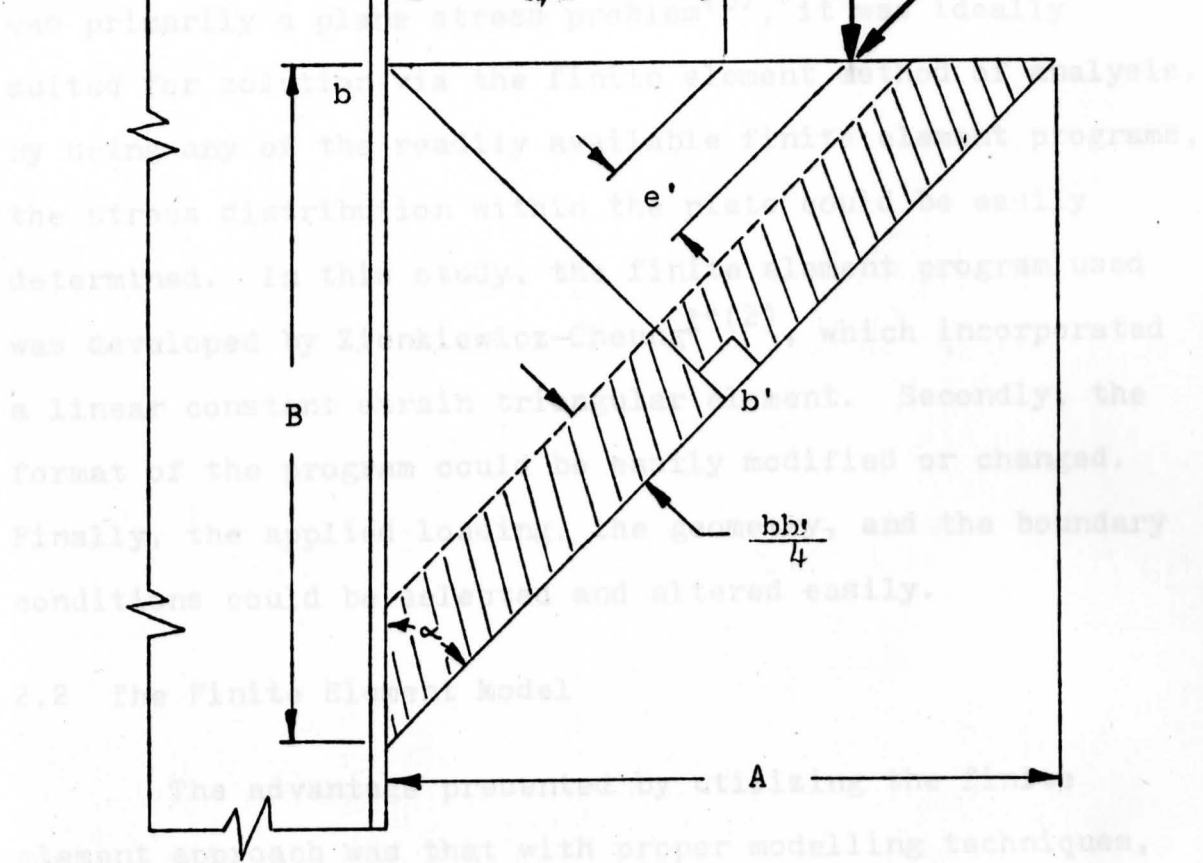


Fig. 1.7. Current Buckling Consideration

Hereafter referred to as I-C.

See Appendix A for listing of program.

- - - - -

CHAPTER TWO

DETERMINING THE FINITE ELEMENT MODEL AND PRELIMINARY TESTING FOR ACCURACY

2.1 Selection of Finite Element Computer Program

Since the analysis of the triangular stiffener plate was primarily a plane stress problem⁽⁵⁾, it was ideally suited for solution via the finite element method of analysis. By using any of the readily available finite element programs, the stress distribution within the plate could be easily determined. In this study, the finite element program used was developed by Zienkiewicz-Cheung^{** (2)}, which incorporated a linear constant strain triangular element. Secondly, the format of the program could be easily modified or changed. Finally, the applied loading, the geometry, and the boundary conditions could be selected and altered easily.

2.2 The Finite Element Model

The advantage presented by utilizing the finite element approach was that with proper modelling techniques, complex bodies could be analyzed both quickly and accurately. It became necessary to carefully determine the best possible

* Hereafter referred to as Z-C.

** See Appendix A for listing of program.

model in order to accurately determine the stresses throughout the triangular plate.

2.2.1 The Element Configuration and Building Code

Due to limitations imposed in the Z-C program, the maximum number of elements was limited to one hundred (100). The two configurations shown in Figure 2.1 were found to be the most consistent and symmetrical in their arrangement for the triangular plate problem.

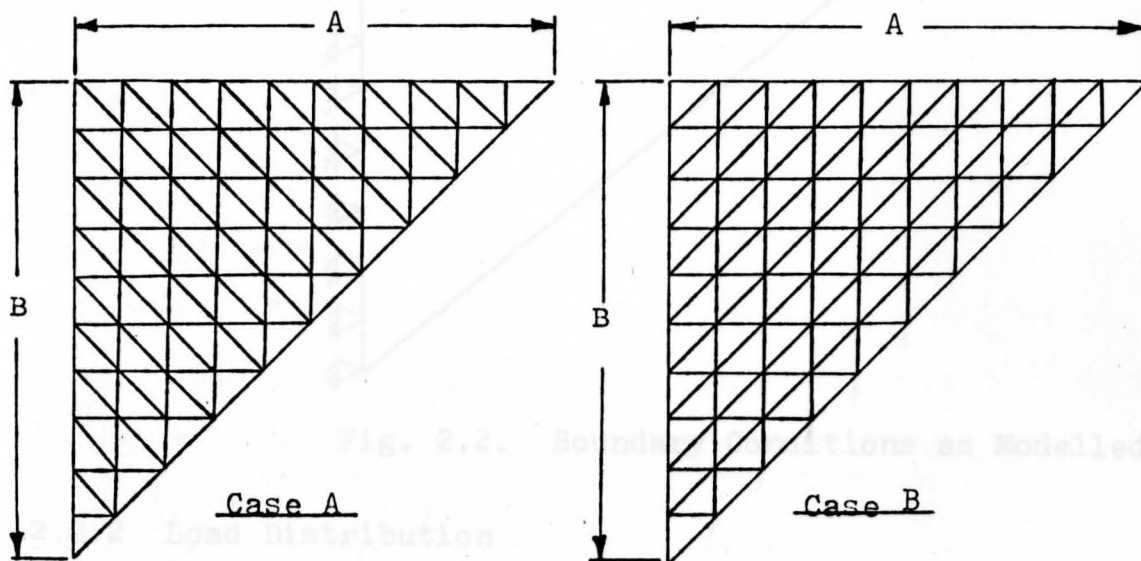


Fig. 2.1. Possible Configurations

Despite the choice for the configuration, the boundary conditions had to be established. By using the displacement criteria established in the experimental⁽⁴⁾ and theoretical⁽³⁾ works, translations were taken as zero in x

and y directions along the supported edge and in the x direction along the loaded edge. The boundary conditions were thus established. These are illustrated in Figure 2.2. Note that rotational displacements have no real meaning in the plane stress approach.

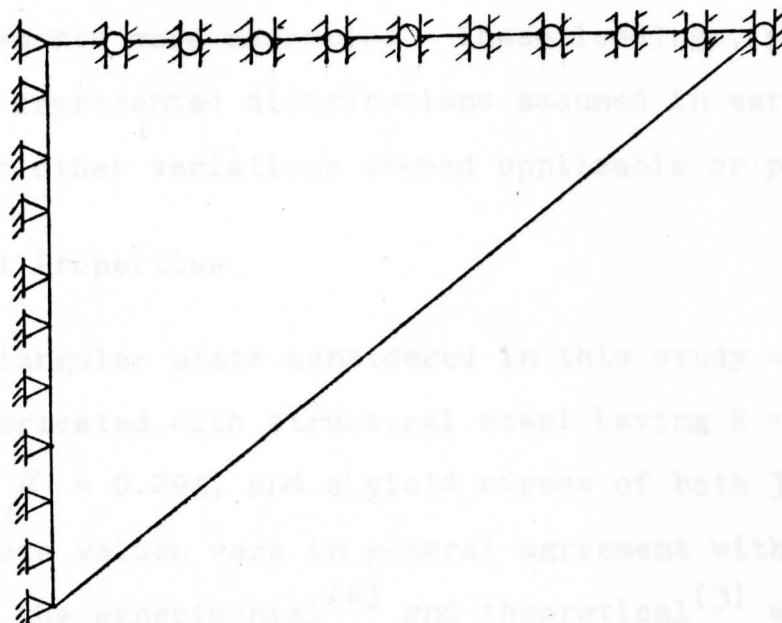


Fig. 2.2. Boundary Conditions as Modelled

2.2.2 Load Distribution

Perhaps the most important parameter in the analysis of the triangular plate was the distribution of load across the loaded edge. Current design practice⁽⁷⁾ was to assume a uniform distribution and ignore any concentrations. However, in both the experimental⁽⁴⁾ and theoretical⁽³⁾ works, it has been found that this was not the case, but rather a special case. The load distributions assumed, calculated or measured

in past studies were functions of the type of load, the supported beam stiffness, the adequacy of the welds, and initial crookedness. With all the variables to consider, it becomes extremely difficult to determine how the plate stresses vary with a corresponding change in the load distribution.

In order to determine the degree of variance in stress effects for various loading conditions, a series of loading arrangements were assembled. These loadings, presented in Figure 2.3, represented distributions assumed in earlier approaches plus other variations deemed applicable or possible.

2.2.3 Material Properties

The triangular plate considered in this study was taken to be fabricated with structural steel having $E = 29,500$ KSI and $\mu = 0.295$, and a yield stress of both 36 KSI or 50 KSI. These values were in general agreement with those taken in the experimental⁽⁴⁾ and theoretical⁽³⁾ works. It was not intended to limit the applicability of this study by using only steel, but rather to obtain results easily verified by the earlier studies⁽³⁾⁽⁴⁾.

2.2.4 Preliminary Testing to Determine the Extent of Stress Variation Due to a Variation in the Load Distribution

Since the previous studies⁽³⁾⁽⁴⁾ demonstrated that the buckling phenomena was dependent upon the maximum free edge stress and its location, it was necessary to determine the variation in the maximum stress and its location for

(upper numerical values indicate percent of total load distribution at that node. Lower numerical values indicate node numbers)

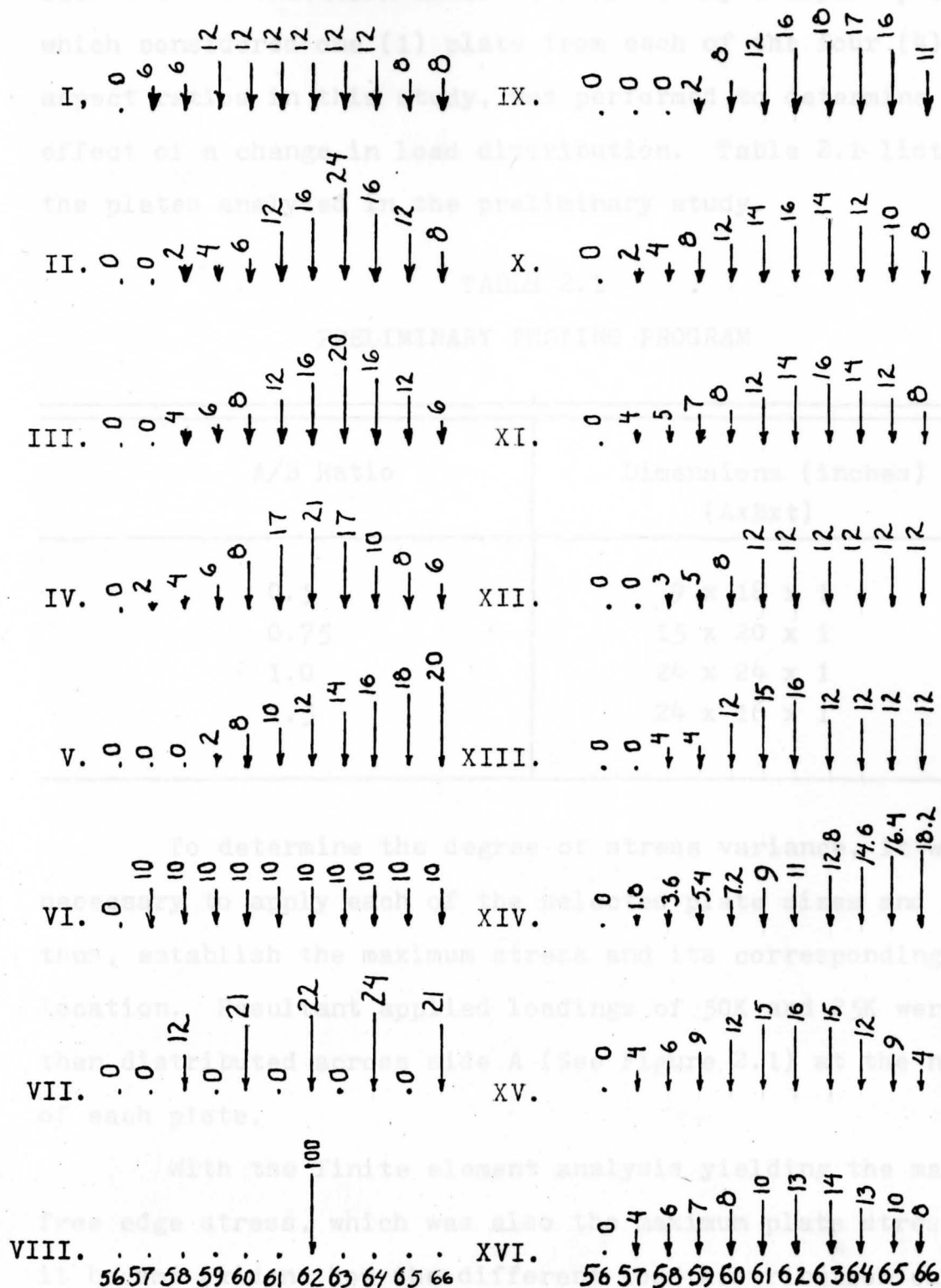


Fig. 2.3. Load Distribution Cases (upper numerical values indicate percent of total load distribution at that node. Lower numerical values indicate node numbers)

each load distribution case. A preliminary analysis program, which considered one (1) plate from each of the four (4) aspect ratios in this study, was performed to determine the effect of a change in load distribution. Table 2.1 lists the plates analyzed in the preliminary study.

TABLE 2.1
PRELIMINARY TESTING PROGRAM

A/B Ratio	Dimensions (inches) (AxBxt)
0.5	9 x 18 x 1
0.75	15 x 20 x 1
1.0	24 x 24 x 1
1.5	24 x 16 x 1

To determine the degree of stress variance, it was necessary to apply each of the selected plate sizes and thus, establish the maximum stress and its corresponding location. Resultant applied loadings of 50K and 25K were then distributed across side A (See Figure 2.1) at the nodes of each plate.

With the finite element analysis yielding the maximum free edge stress, which was also the maximum plate stress, it became evident how the different load distribution cases affected the stress distribution. This is illustrated in Figure 2.4 for the 24" x 24" x 1" plate. By discarding

those cases which produced large stress concentrations in elements along the loaded edge, say directly beneath an applied concentrated load, and those which were considered impractical, it was found that the variation in the maximum free edge stress for each aspect ratio fell within a narrow range for most applied load distribution cases (See Figure 2.4). This type of distribution was also evident in the plates tested from the other aspect ratios; i.e., the variation in the magnitude of the maximum stress fell within a similar narrow range.

Based upon the results of the preliminary analysis, it was concluded that the stress distribution within the triangular plate was not entirely (or predominantly) controlled by the load distribution chosen. Case 3 (See Figure 2.3) was then selected to represent the load distribution in the subsequent analysis with Case 10 and Case 15 used for verification. These were chosen since they represented the average, minimum, and maximum stress as demonstrated by the stress ranges shown in Figure 2.4.

2.2.5 Final Selection of the Model Configuration

With the boundary conditions, material properties and load distributions established, the two trial model configurations were then analyzed in order to determine which more closely simulated the experimental results⁽⁴⁾. Important comparisons between the finite element analysis and the experimental results were thought to be:

- 1.) The magnitude and sign of the maximum free edge stress.
- 2.) The location of the maximum free edge stress (See Figure 2.5).

A plate with an aspect ratio of 1.0 and dimensions of 30" x 30" x $\frac{1}{4}$ " was chosen for comparison as this size was also tested by Buettner and O'Sheridan⁽⁴⁾.

Resultant loadings equal in magnitudes to the applied loads used on on Buettner and O'Sheridan's experimental 30" x 30" x $\frac{1}{4}$ " plate were applied to the finite element models using load Case 3. Table 2.3 illustrates a comparison between the analysis of the two models and the experimental counterpart. Slight variations between the SR-4 strain guage and finite element stresses were not considered critical since strain gauges are often affected by a host of conditions which cannot always be exactly controlled. Also, it has been shown that a slight variation in stress levels exists when the load distribution varies (See Figure 2.4).

It is evident from Table 2.3 that Case B modelled the experimental triangular plate stress levels and their directions accurately. However, Case A modelled neither the stress levels nor their directions.

Before the selection of the finite element model could be finalized, it was necessary to consider the second important comparison; i.e., the location of the maximum free edge stress. The experimental⁽⁴⁾ and the theoretical⁽³⁾ studies demonstrated that the position of the maximum free edge stress is constant within each aspect ratio. In order to determine the location of the maximum free edge stress

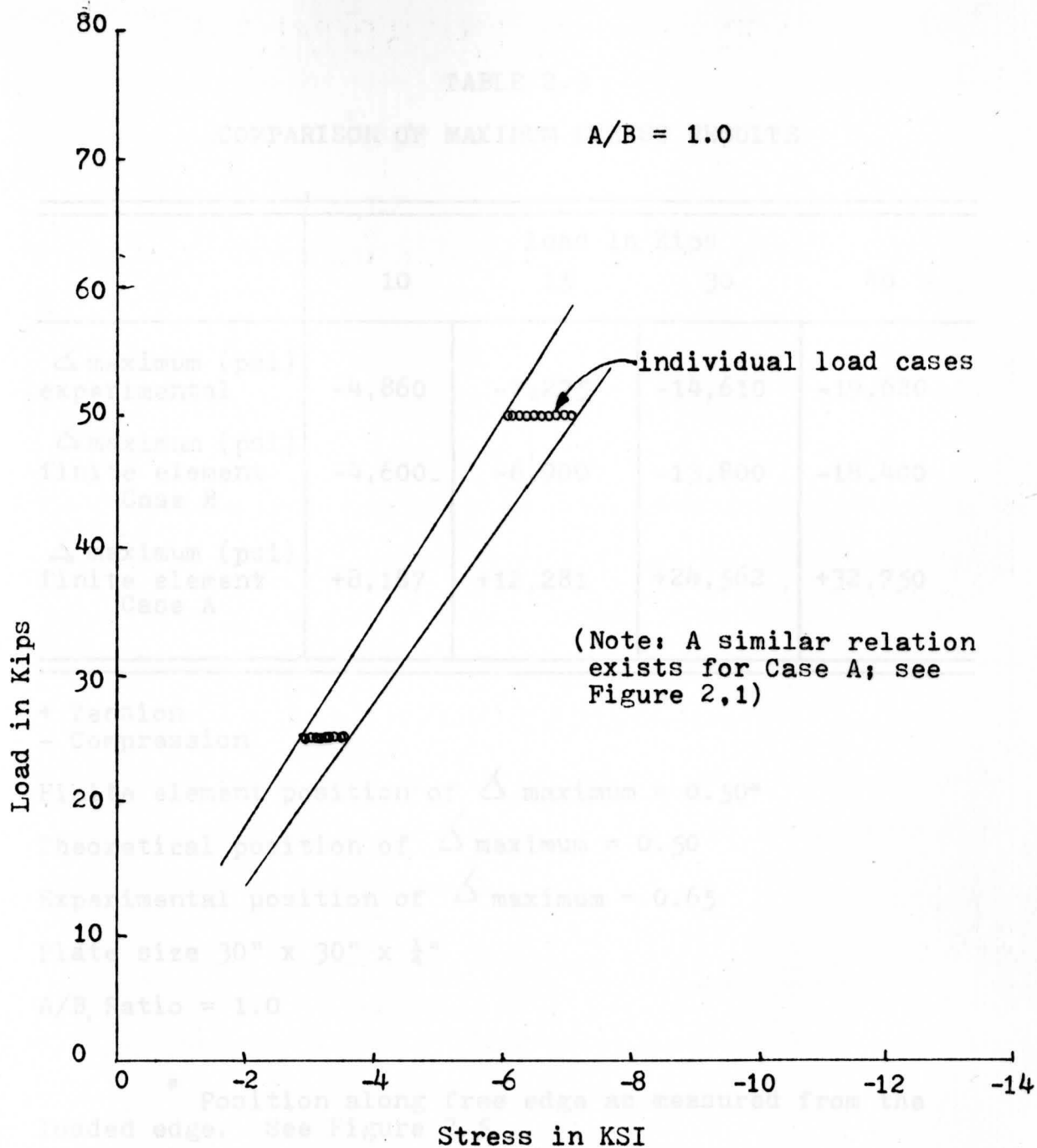


Fig. 2.4. Load Case Stress Variance
(Graph shown is for Configuration B; Figure 2.1)

TABLE 2.3
COMPARISON OF MAXIMUM STRESS RESULTS

	Load In Kips			
	10	15	30	40
Δ maximum (psi) experimental	-4,860	-7,275	-14,610	-19,620
Δ maximum (psi) finite element Case B	-4,600	-6,900	-13,800	-18,400
Δ maximum (psi) finite element Case A	+8,187	+12,281	+24,562	+32,750

+ Tension
- Compression

Finite element position of Δ maximum = 0.50*

Theoretical position of Δ maximum = 0.50

Experimental position of Δ maximum = 0.65

Plate size 30" x 30" x $\frac{1}{4}$ "

A/B Ratio = 1.0

* Position along free edge as measured from the loaded edge. See Figure 2.5.

within the models, one (1) plate from each of the four (4) aspect ratios was loaded with applied resultants of 40K using load Cases 3, 10, and 15 (See Figure 2.3). Table 2.2 (See also Figure 2.5) presents a comparison of the finite element locations of the maximum free edge stress for the various aspect ratios along with the results of Salmon's and Buettnner and O'Sheridan's earlier studies. Note, however, that even though solutions using configurations A and B gave oppositely sensed stresses, the locations of the maximum free edge stresses were the same for both configurations. Based upon these comparisons, configuration A was eliminated from further consideration. Configuration B was found to model both the stress levels and the respective locations accurately and, thus, was chosen as the sole finite element model throughout the study. It is for this reason that Figure 2.6 was presented.

2.3 Scope of the Analysis Program

Twenty different plate sizes were analyzed, with the range of sizes falling into four (4) aspect ratios: 0.5, 0.75, 1.0, and 1.5. These sizes and ranges were thought to be representative of those commonly used in structural practice. The actual plate dimensions chosen permitted enough deviation so that any relationship existing between the plate sizes would become easily noticeable. Table 2.4 gives a listing of the plate sizes that were analyzed.

TABLE 2.2
 MAXIMUM FREE EDGE STRESS
 AS A RATIO OF D/C

A/B Ratio	* Finite Element D/C	Salmon D/C	Experimental D/C
0.5	0.25	-	-
0.75	0.40	0.40	0.50
1.0	0.50	0.50	0.65
1.5	0.65	0.85	0.90

* Case A and Case B both exhibited their maximum free edge stress at the same locations.

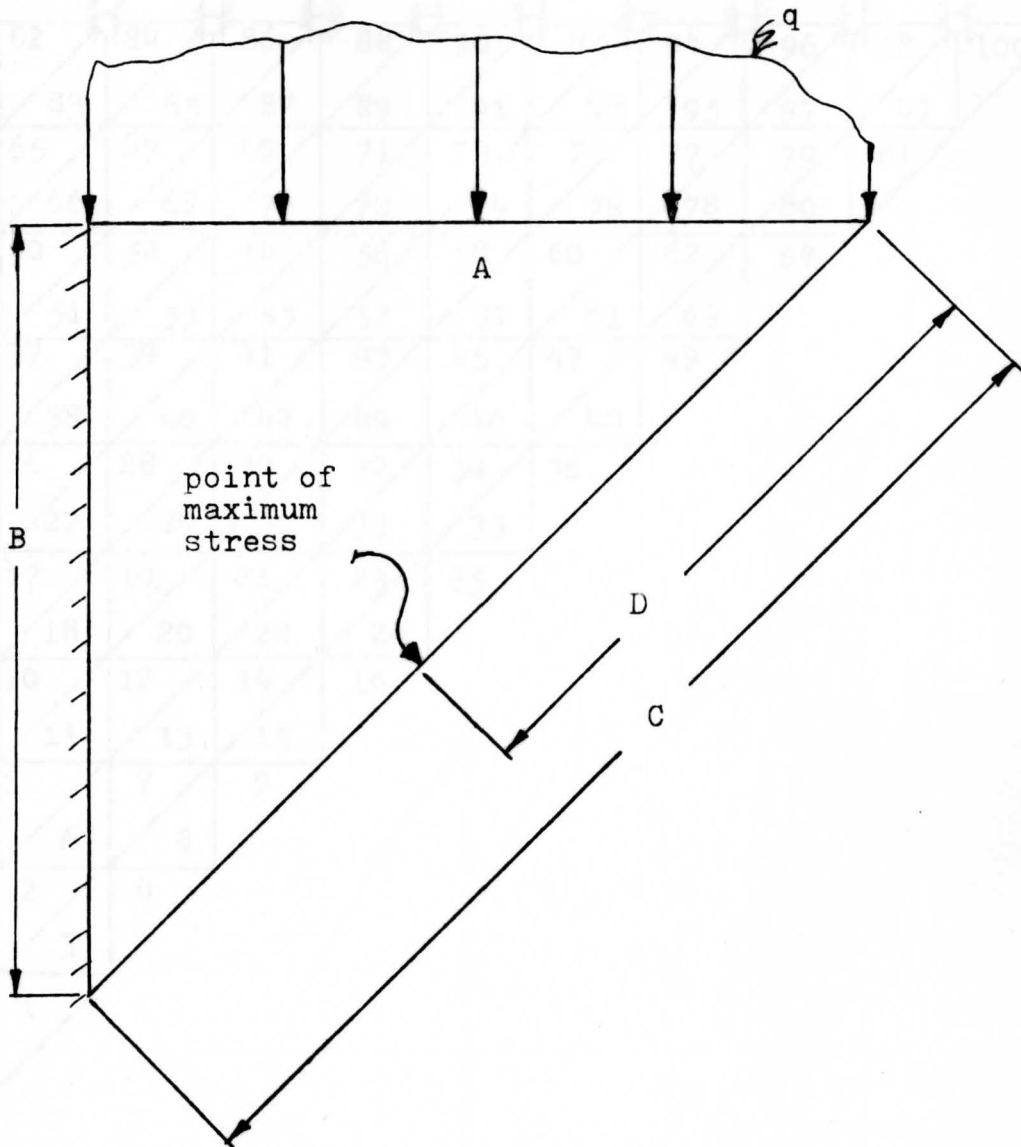


Fig. 2.5. Free Edge Stress Location

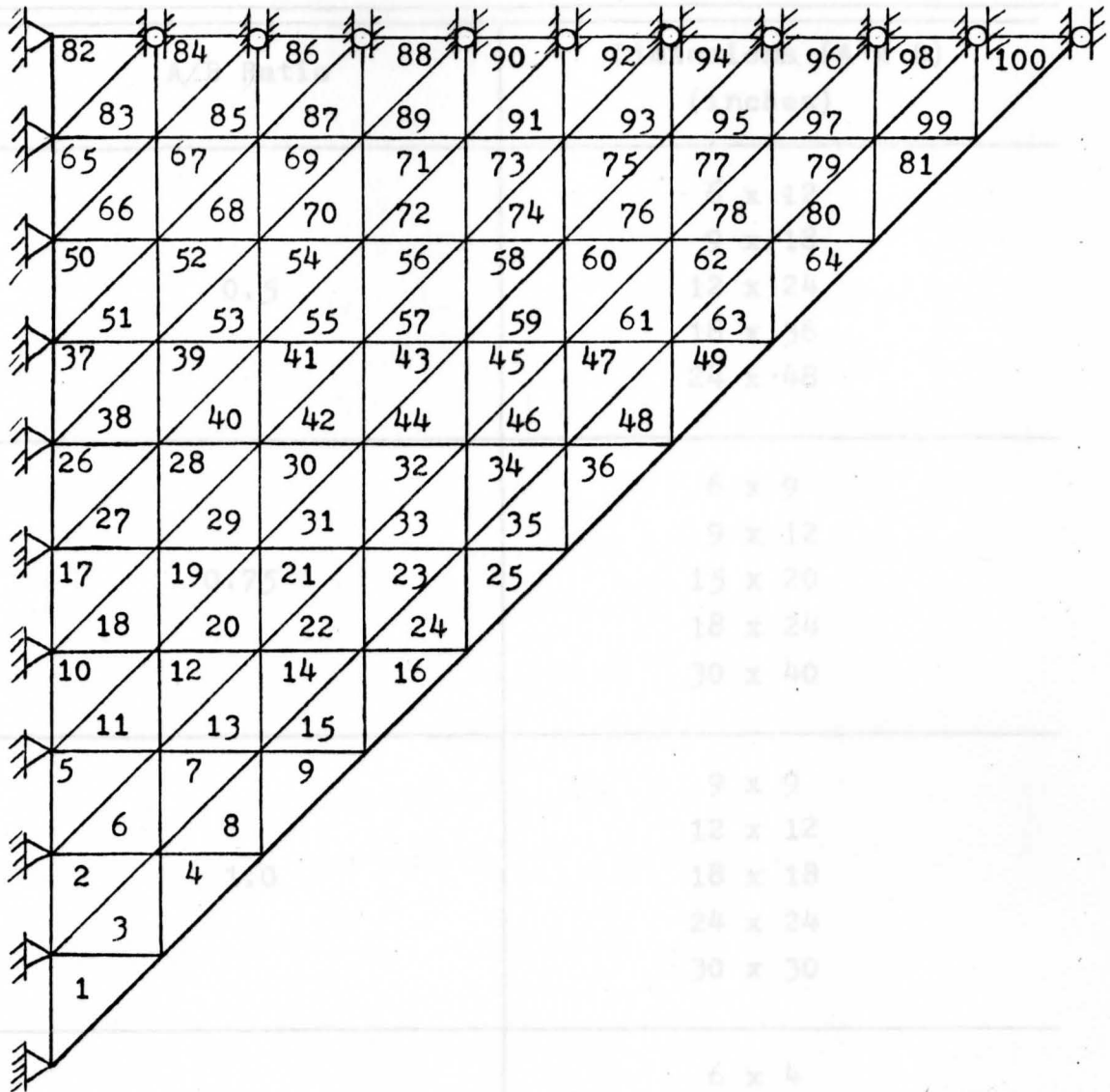


Fig. 2.6. The Finite Element Model and Element Numbering (See Appendix A)

TABLE 2.4

PLATE TESTING SCHEDULE

A/B Ratio	Dimensions (A x B) (inches)
0.5	6 x 12 9 x 18 12 x 24 18 x 36 24 x 48
0.75	6 x 9 9 x 12 15 x 20 18 x 24 30 x 40
1.0	9 x 9 12 x 12 18 x 18 24 x 24 30 x 30
1.5	6 x 4 15 x 10 18 x 12 36 x 24 30 x 20

- - - - -

CHAPTER 3

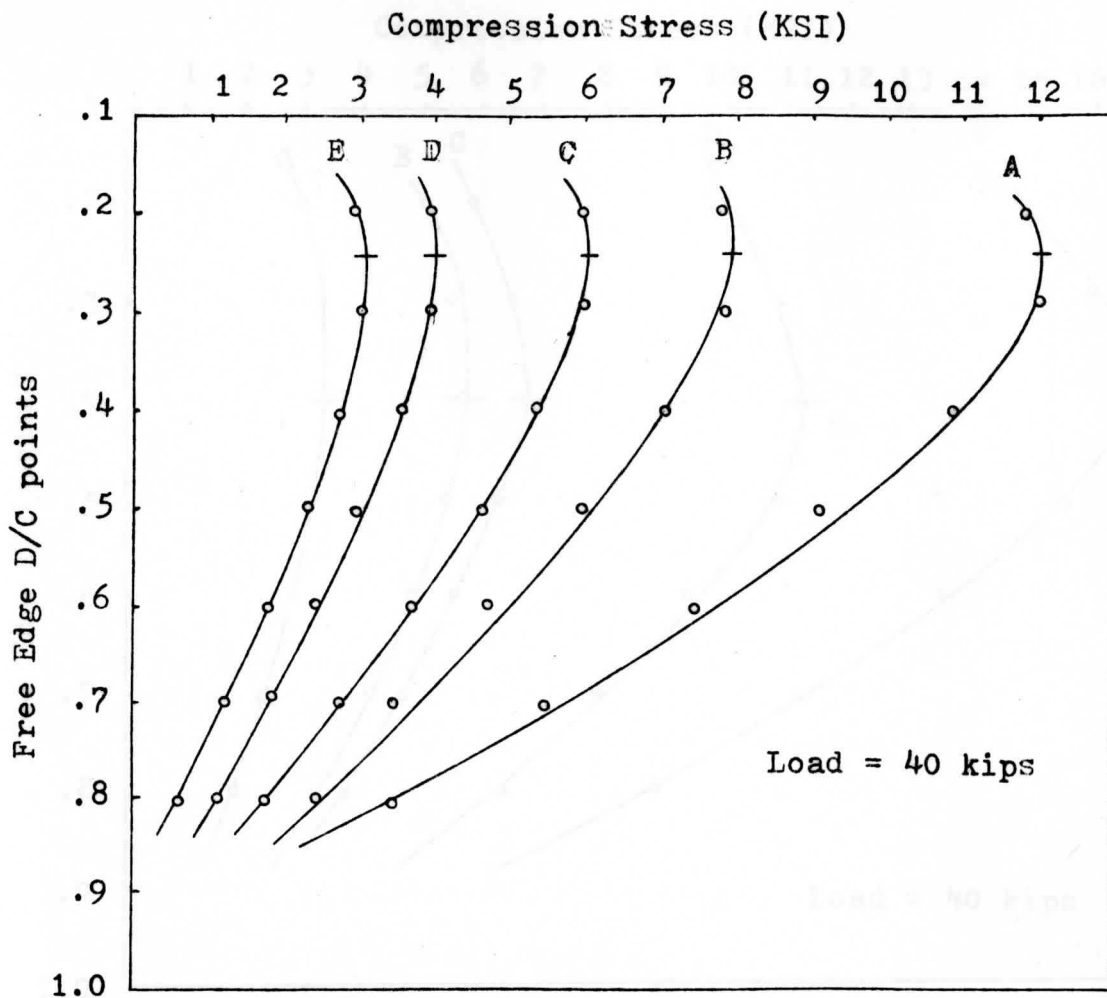
PRESENTATION OF RESULTS

3.1 Final Analysis

The preliminary analysis program established the accuracy and the selection of the finite element model. It became necessary to then expand the investigation for all the aspect ratios and plate sizes listed previously in Table 2.2. The total (resultant) load application consisted of a 40 kip load distributed at the nodes along Side A (See Figure 2.2) using the distribution designated as Case 3 in Figure 2.3. Only one load application was necessary per plate since the finite element analysis is linear and elastic; i.e., the results for a 20 kip applied resultant load is one half that for the 40 kip load, and so on.

3.2 Results

The results of the expanded analysis program are presented in Figures 3.1 through 3.4 inclusive. These curves represent the longitudinal free edge stress distribution; i.e., stress in a direction parallel to the free edge, and indicate the location of this maximum longitudinal stress for all of the plates considered under the action of a 40 kip load, distributed as noted earlier. These plots verify that the location of the



A/B Ratio = 0.50
 Thickness = 1.0 inch

Fig. 3.1. Longitudinal Free Edge
 Stress Distribution

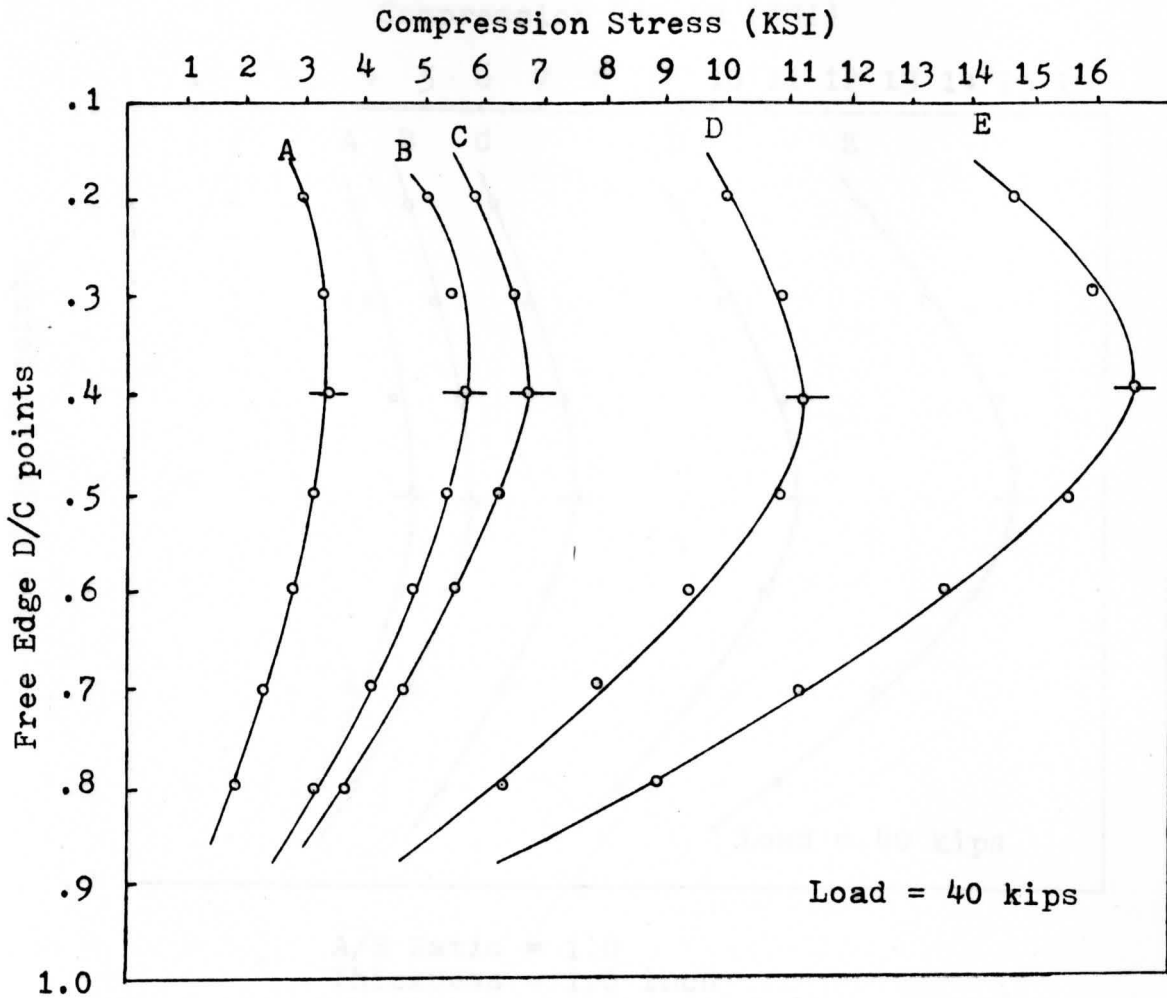
A--6" x 12"

B--9" x 18"

C--12" x 24"

D--18" x 36"

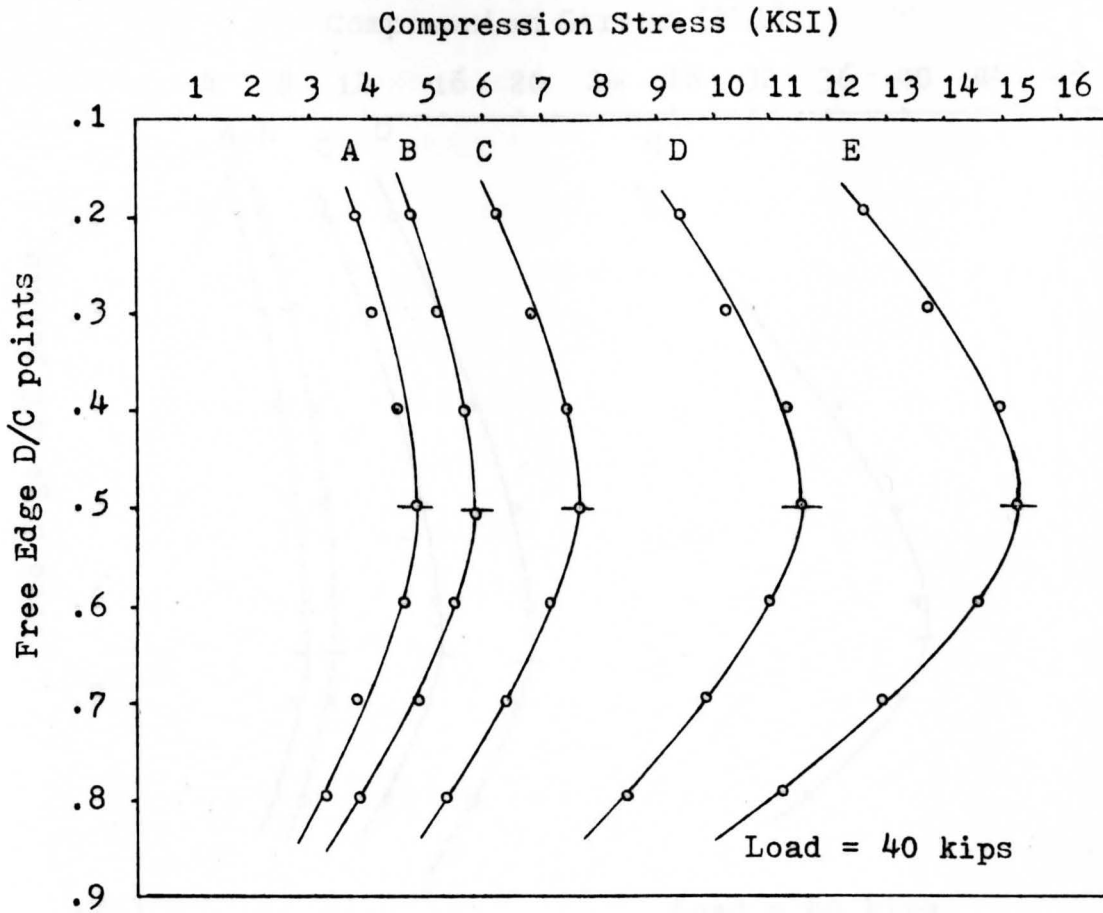
E--24" x 48"



A/B Ratio = 0.75
Thickness = 1.0 inch

Fig. 3.2 Longitudinal Free Edge
Stress Distribution

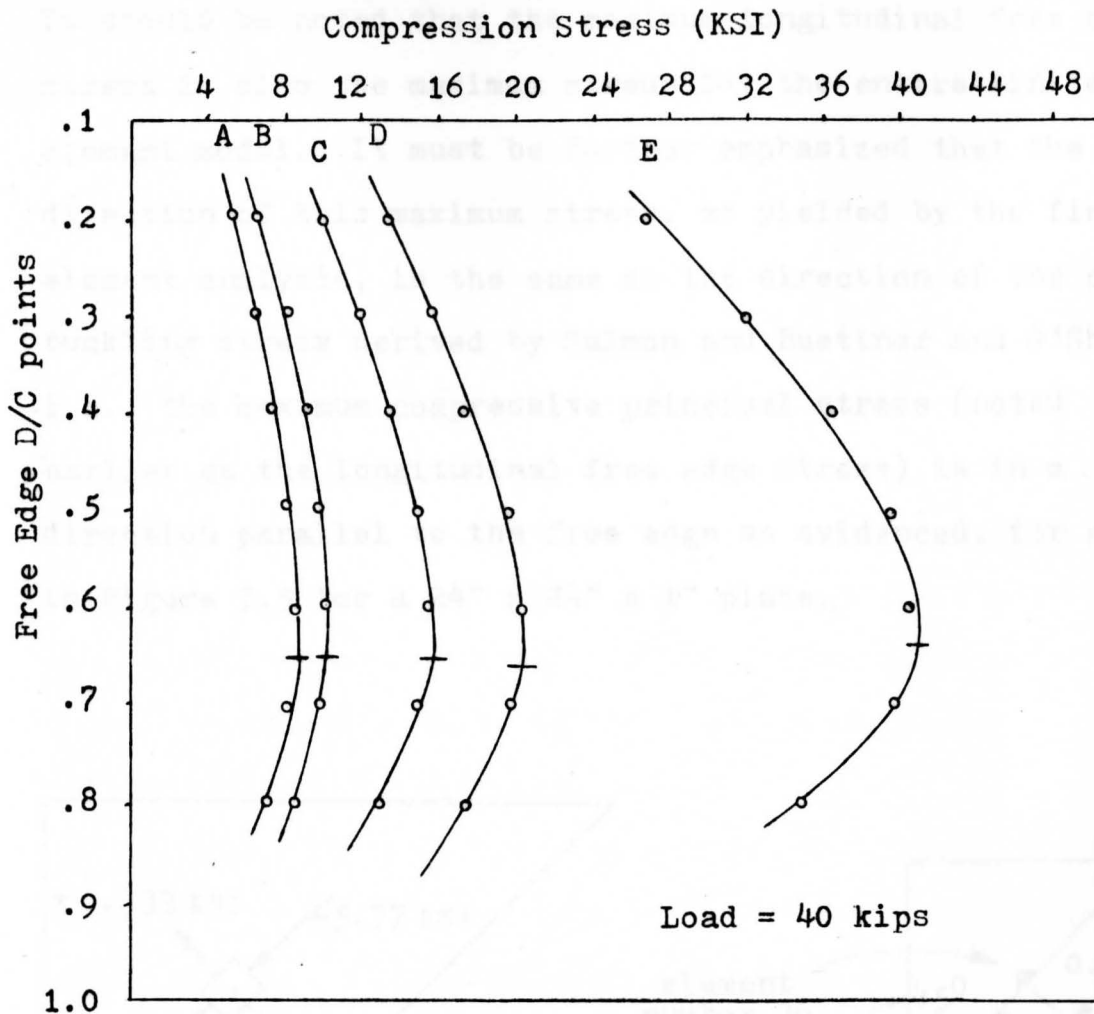
A--30' x 40"
B--18" x 24"
C--15" x 20"
D--9" x 12"
E--6" x 8"



A/B Ratio = 1.0
Thickness = 1.0 inch

Fig. 3.3 Longitudinal Free Edge
Stress Distribution

- A--30" x 30"
B--24" x 24"
C--18" x 18"
D--12" x 12"
E--9" x 9"



A/B Ratio = 1.5
 Thickness = 1.0 inch

Fig. 3.4. Longitudinal Free Edge
 Stress Distribution

- A--30" x 20"
- B--24" x 16"
- C--18" x 12"
- D--12" x 8"
- E--6" x 4"

maximum free edge stress is constant for any aspect ratio. It should be noted that the maximum longitudinal free edge stress is also the maximum stress for the entire finite element model. It must be further emphasized that the direction of this maximum stress, as yielded by the finite element analysis, is the same as the direction of the critical buckling stress derived by Salmon and Buettner and O'Sheridan; i.e., the maximum compressive principal stress (noted earlier as the longitudinal free edge stress) is in a direction parallel to the free edge as evidenced, for example, in Figure 3.5 for a 24" x 24" x 1" plate.

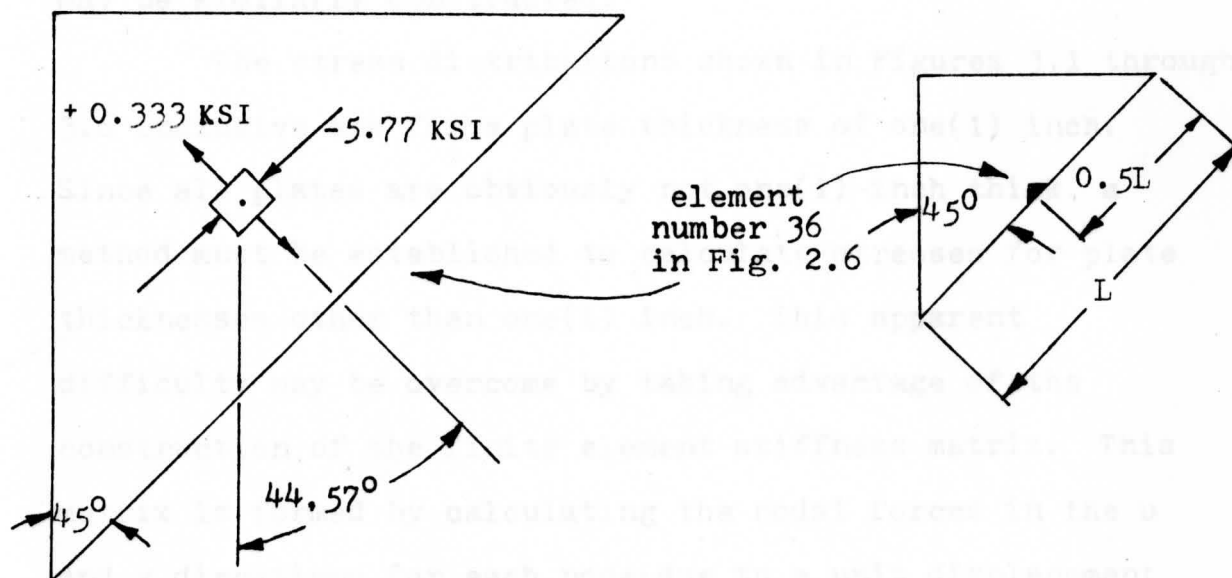


Fig. 3.5. Maximum Longitudinal Stress Directions

An important relationship extracted from the graphical presentations is that the free edge stress is inversely proportional to the loaded edge length(A); i.e., the edge stress is doubled when the loaded edge length(A) is halved. For example, in Figure 3.3 the maximum stress for a 9" x 9" x 1" plate is 15.4 KSI, while the maximum stress for an 18" x 18" x 1" stress is 7.7 KSI.

Since linearity exists between different resultant loads on an individual plate, the relationships between the free edge stress levels and the loaded edge length(A) may be utilized more practically as illustrated in Figure 3.5 for an A/B ratio of 1.0 and a plate thickness equal to one(1) inch. Note that the plots for other aspect ratios may be similarly constructed.

The stress distributions shown in Figures 3.1 through 3.6 inclusive are for a plate thickness of one(1) inch. Since all plates are obviously not one(1) inch thick, a method must be established to calculate stresses for plate thicknesses other than one(1) inch. This apparent difficulty may be overcome by taking advantage of the construction of the finite element stiffness matrix. This matrix is formed by calculating the nodal forces in the u and v directions for each node due to a unit displacement occurring in the direction of each degree of freedom (See Figure 3.7); e.g., in equation (3.1), which illustrates the stiffness matrix, the u_{11} value is actually the nodal force in the u_1 direction due to a unit displacement in the u_1 direction.

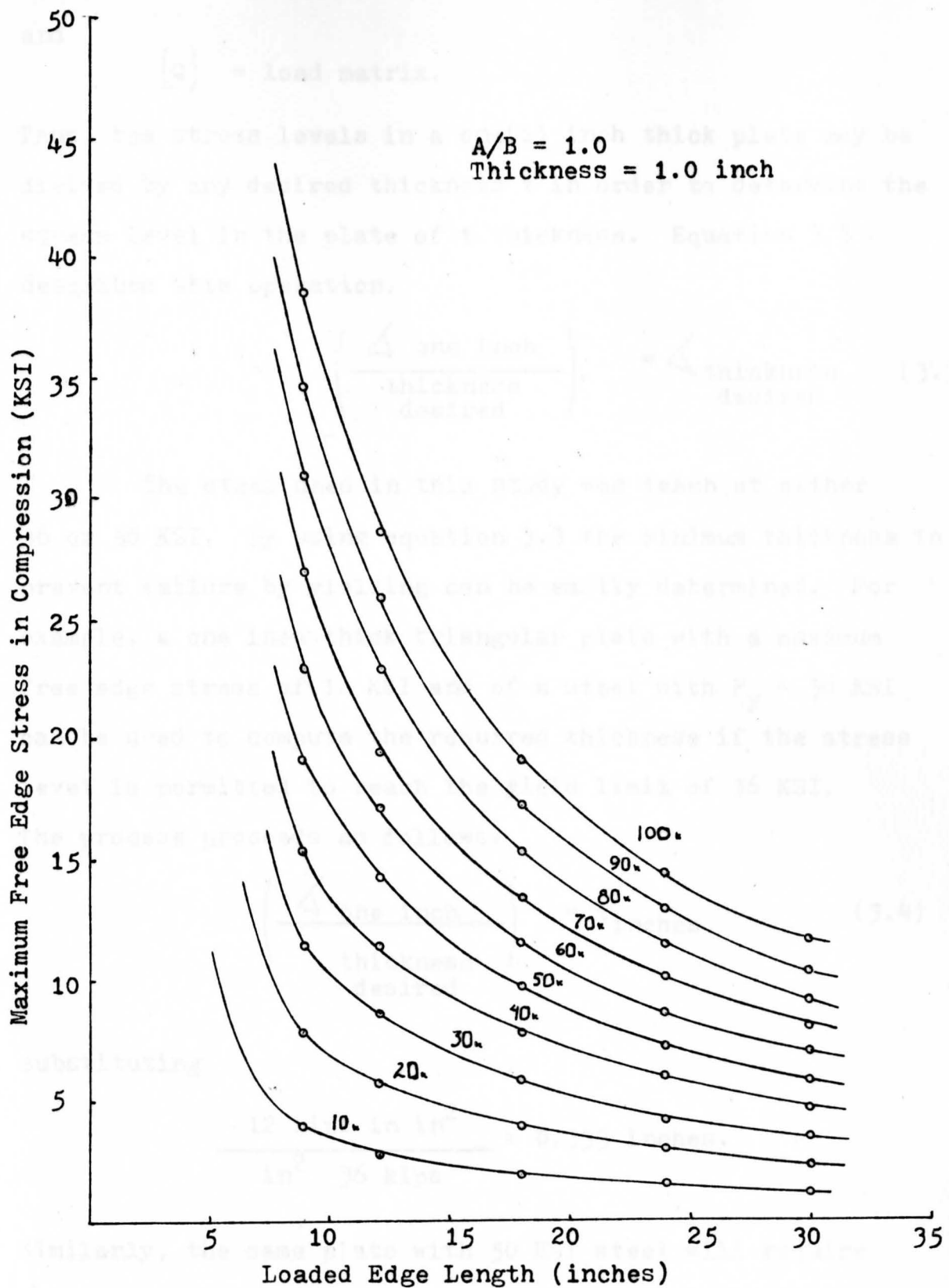


Fig. 3.6. Load Case 3 (Fig. 2.3.)

and

$\{Q\}$ = load matrix.

Thus, the stress levels in a one(1) inch thick plate may be divided by any desired thickness t in order to determine the stress level in the plate of t thickness. Equation 3.3 describes this operation.

$$\left(\frac{\triangle \text{ one inch}}{\text{thickness desired}} \right) = \triangle \text{ thickness desired} \quad (3.3)$$

The steel used in this study was taken at either 36 or 50 KSI. By using equation 3.3 the minimum thickness to prevent failure by yielding can be easily determined. For example, a one inch thick triangular plate with a maximum free edge stress of 12 KSI and of a steel with $F_y = 36$ KSI can be used to compute the required thickness if the stress level is permitted to reach the yield limit of 36 KSI.

The process proceeds as follows:

$$\left(\frac{\triangle \text{ one inch}}{\text{thickness desired}} \right) = t_{\text{inches}} \quad (3.4)$$

substituting

$$\frac{12 \text{ kips in in}^2}{\text{in}^2 \cdot 36 \text{ kips}} = 0.333 \text{ inches.}$$

Similarly, the same plate with 50 KSI steel will require a thickness of only 0.24 inches. This relationship can be

expanded and illustrated as a series of curves as shown in Figure 3.8 for an aspect ratio of 1.0 and a yield stress of 36 KSI. Note that the plots for other aspect ratios and yield stresses may be similarly plotted.

However, as the loaded edge increases in length, the stress becomes increasingly smaller (See Figure 3.6) and the thickness based upon yield criteria (See Figure 3.8) also becomes increasingly smaller. At this point, the plate exhibits an increased potential to buckle; i.e., the maximum longitudinal free edge stress for small plate thicknesses may reach the critical buckling stress before the yield stress can be achieved. Therefore, the curve shown in Figure 3.6 has a limited range of application. It was here that the critical buckling stress equation proposed by Salmon⁽³⁾ and verified experimentally by Buettner and O'Sheridan⁽⁴⁾ was introduced. With the maximum longitudinal free edge stress known for a one(1) inch thickness and its relationship to other thicknesses established, the minimum thickness required to prevent failure by buckling can be calculated. Recalling the buckling equation:

$$\Delta_{\text{critical}} = \frac{K}{(A/t)^2} \quad (1.1)$$

where

K = stiffness coefficient (from Figure 1.3)

A = loaded edge length

and

t = plate thickness,

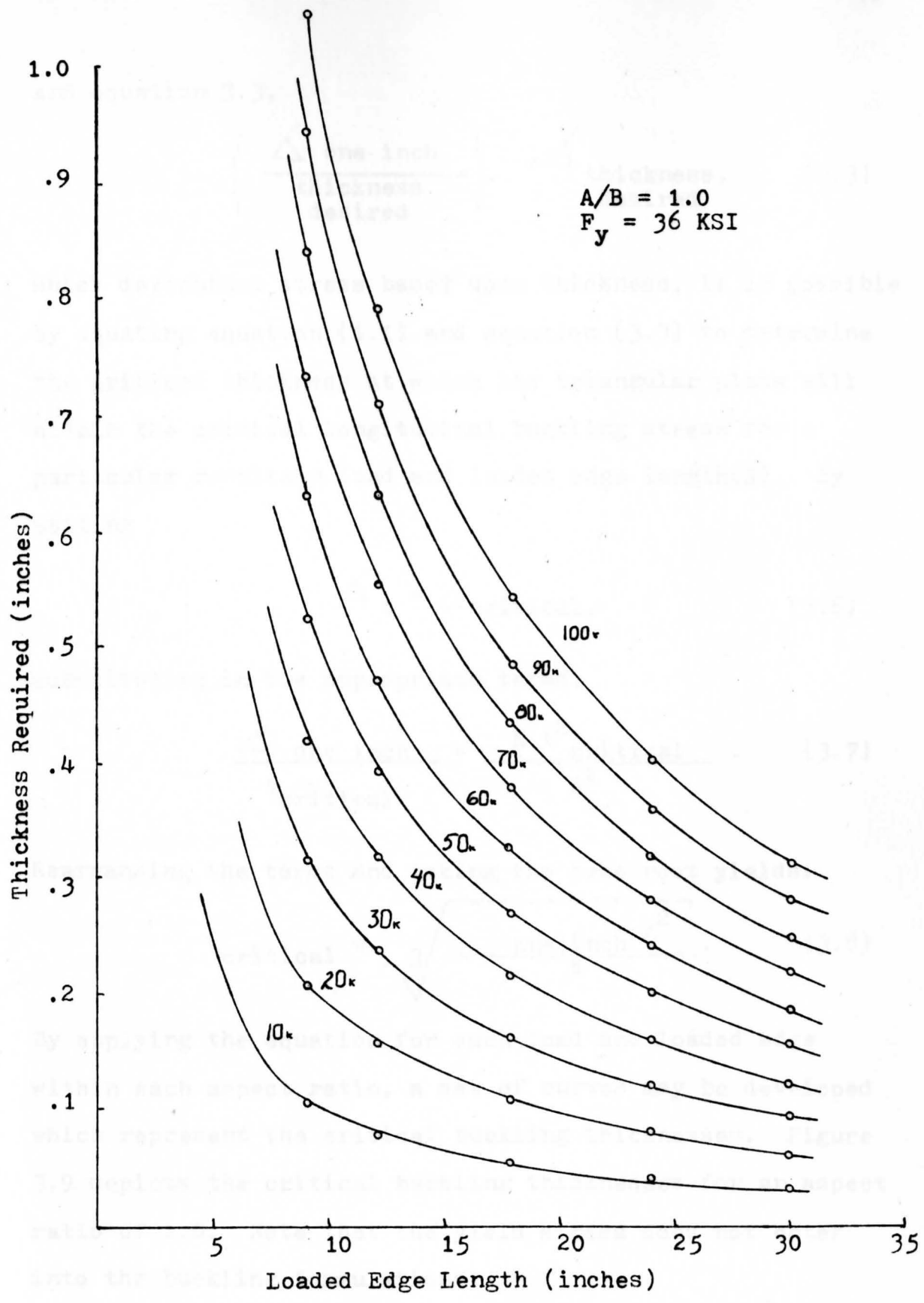


Fig. 3.8. Thickness Based Upon Yield Criteria

and equation 3.3,

$$\left(\frac{\Delta \text{ one inch}}{\text{thickness desired}} \right) = \Delta \text{ thickness, desired} \quad (3.3)$$

which determines stress based upon thickness, it is possible by equating equation (1.1) and equation (3.3) to determine the critical thickness at which the triangular plate will attain the critical longitudinal buckling stress for a particular resultatn load and loaded edge length(A). By setting

$$\Delta_t = \Delta_{\text{critical}}, \quad (3.6)$$

substituting in the appropriate terms,

$$\frac{\Delta \text{ one inch}}{t_{\text{critical}}} = \frac{K t_{\text{critical}}^2}{A^2} \quad (3.7)$$

Rearranging the terms and taking the cube root yields:

$$t_{\text{critical}} = \sqrt[3]{\frac{\text{one inch } A^2}{K}} \quad (3.8)$$

By applying the equation for each load and loaded edge within each aspect ratio, a set of curves may be developed which represent the critical buckling thicknesses. Figure 3.9 depicts the critical buckling thicknesses for an aspect ratio of 1.0. Note that the yield stress does not enter into the buckling formulations.

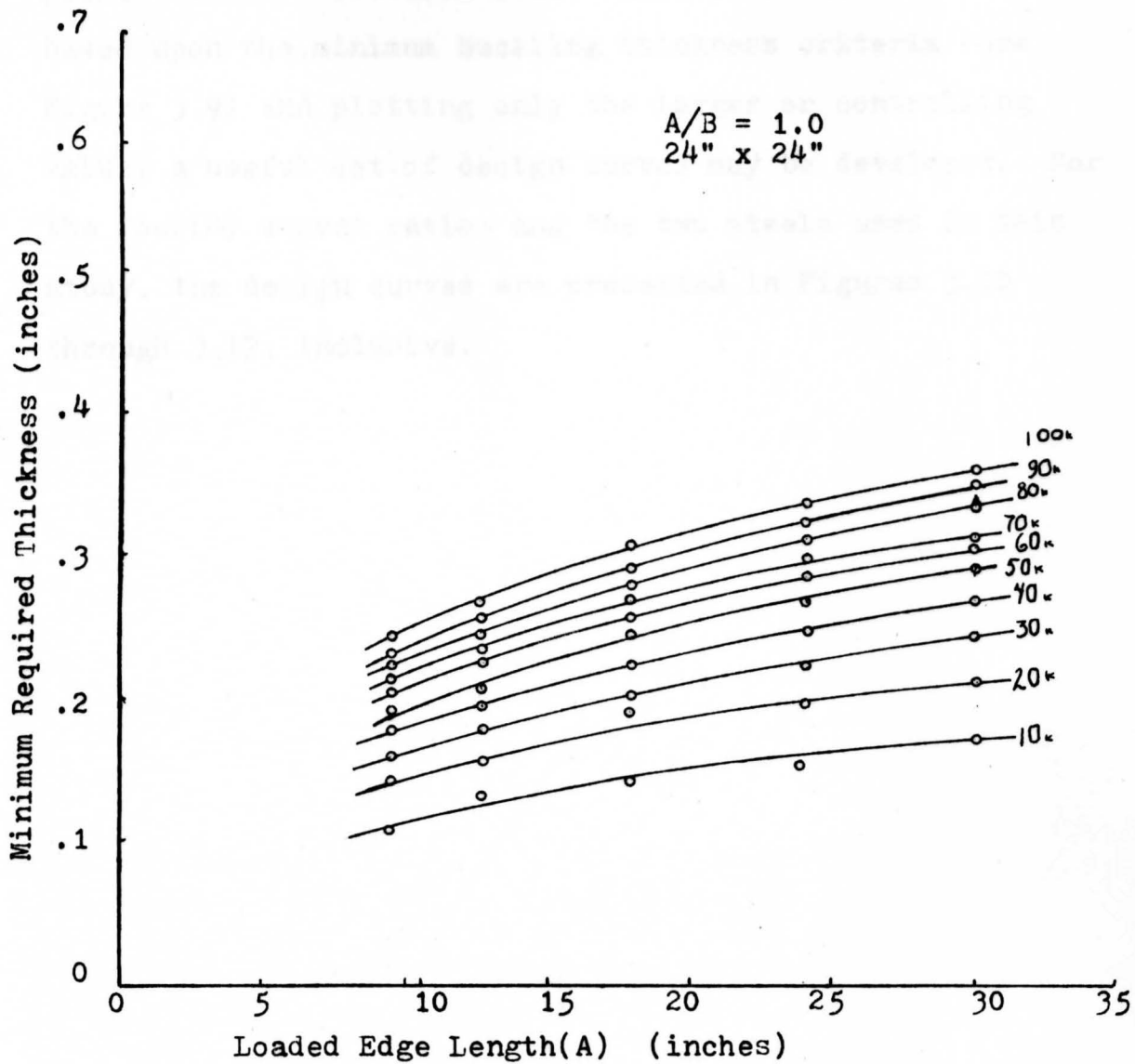


Fig. 3.9. Critical Buckling Thicknesses

By combining the curves based upon the minimum yield thickness criteria (See Figure 3.8) with those based upon the minimum buckling thickness criteria (See Figure 3.9) and plotting only the larger or controlling value, a useful set of design curves may be developed. For the four(4) aspect ratios and the two steels used in this study, the design curves are presented in Figures 3.10 through 3.17, inclusive.



Fig. 3-10. Design Chart: Combined Criteria

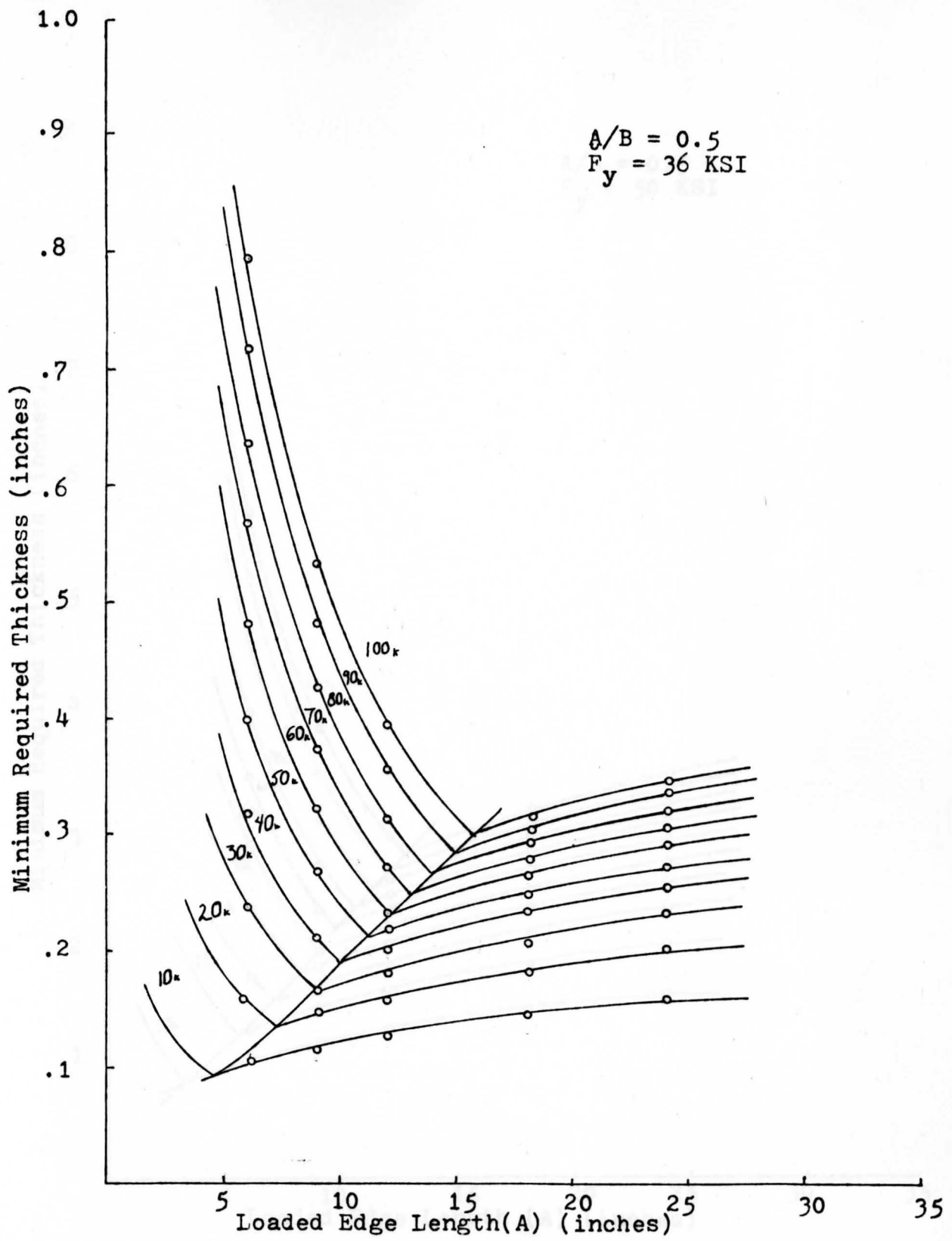


Fig. 3.10. Design Chart: Combined Criteria

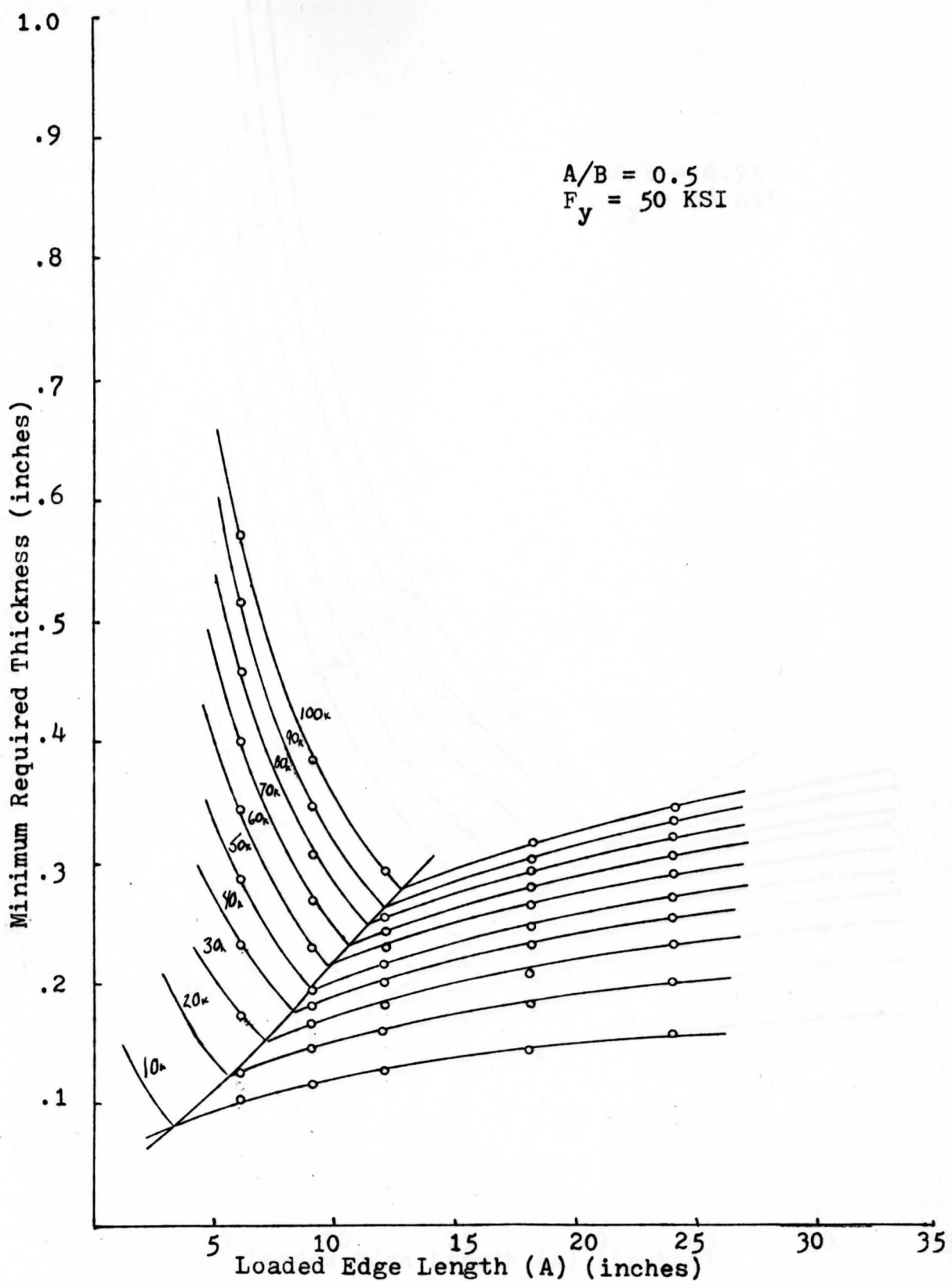


Fig. 3.11. Design Chart: Combined Criteria

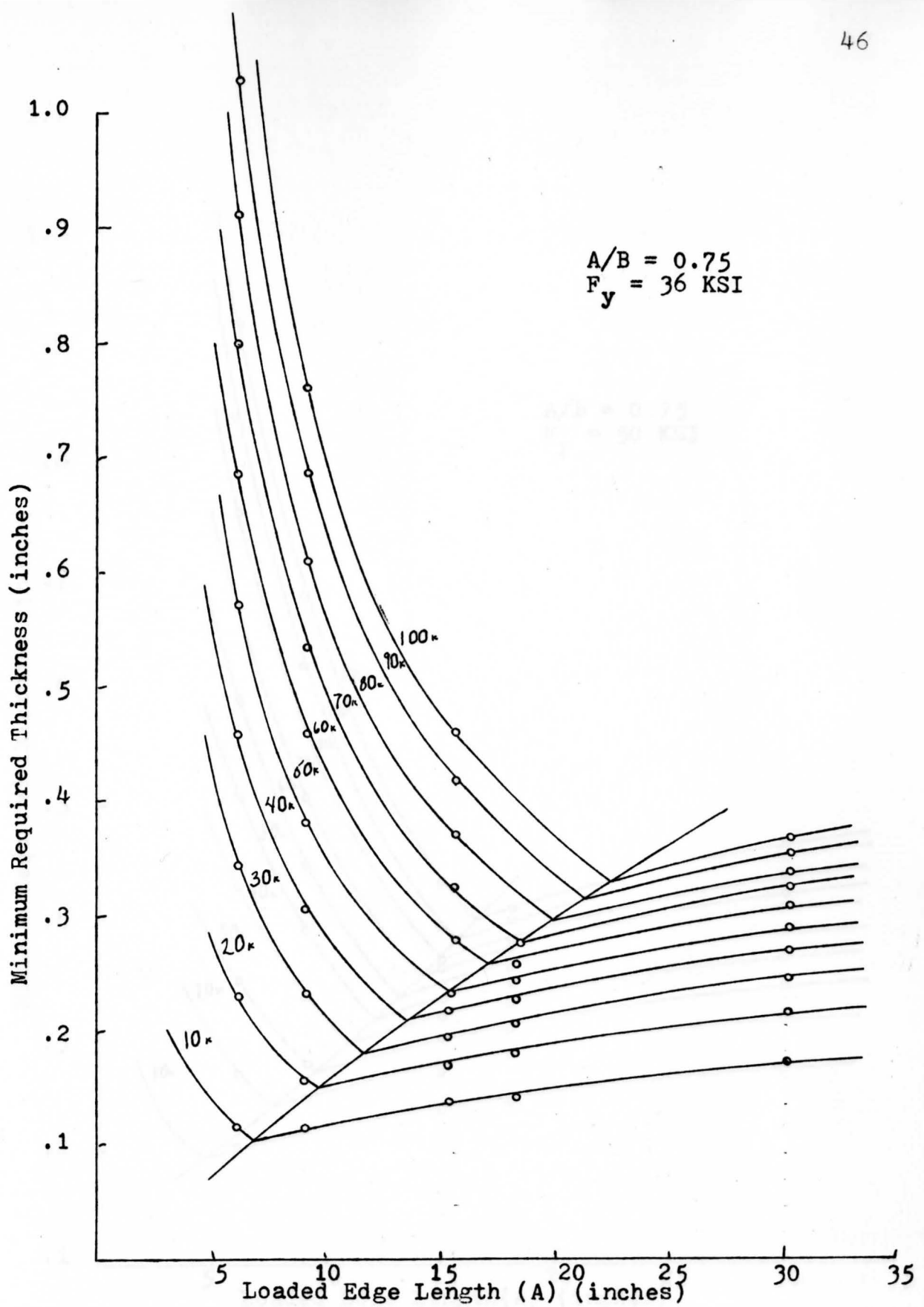


Fig. 3.12. Design Chart: Combined Criteria

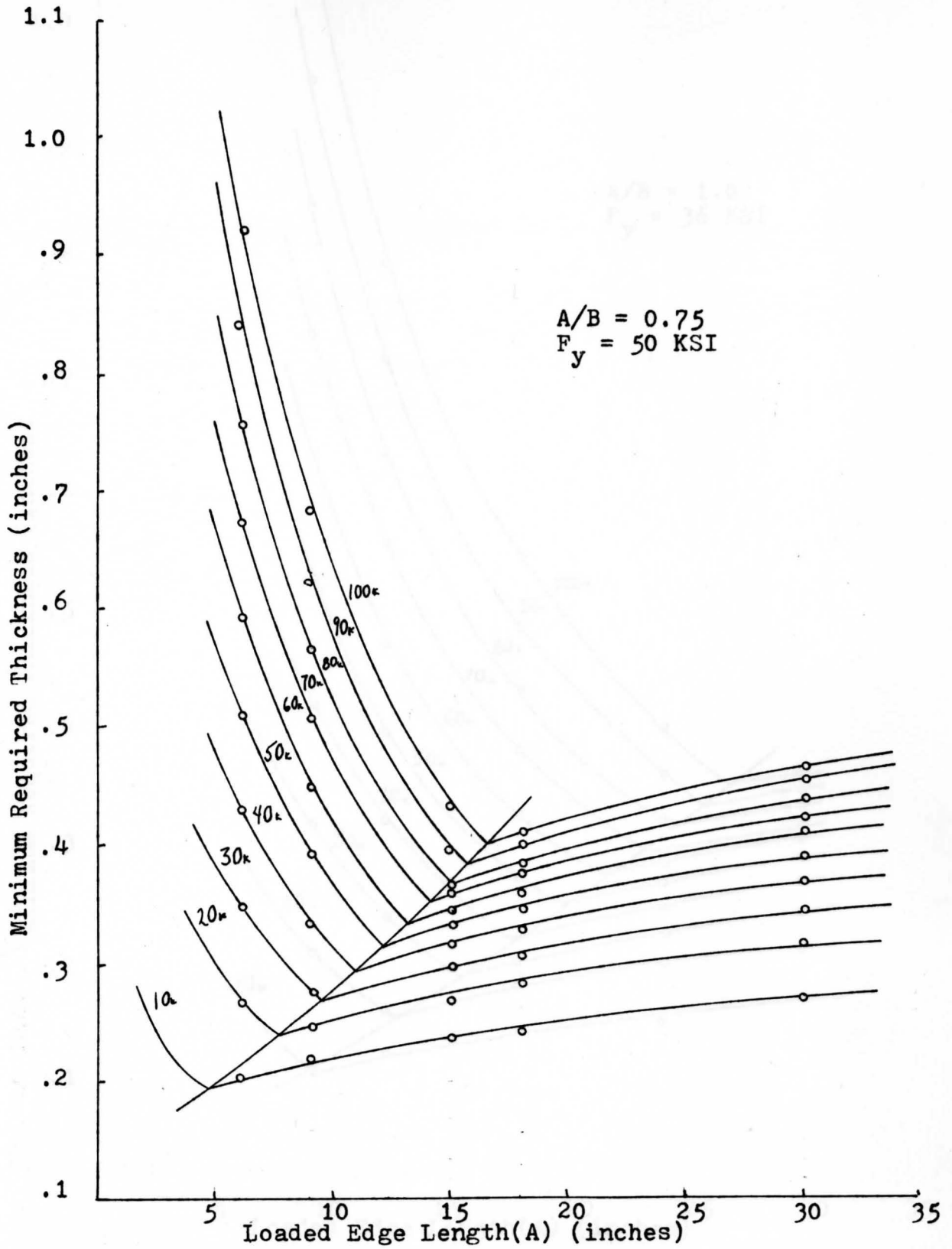


Fig. 3.13. Design Chart: Combined Criteria

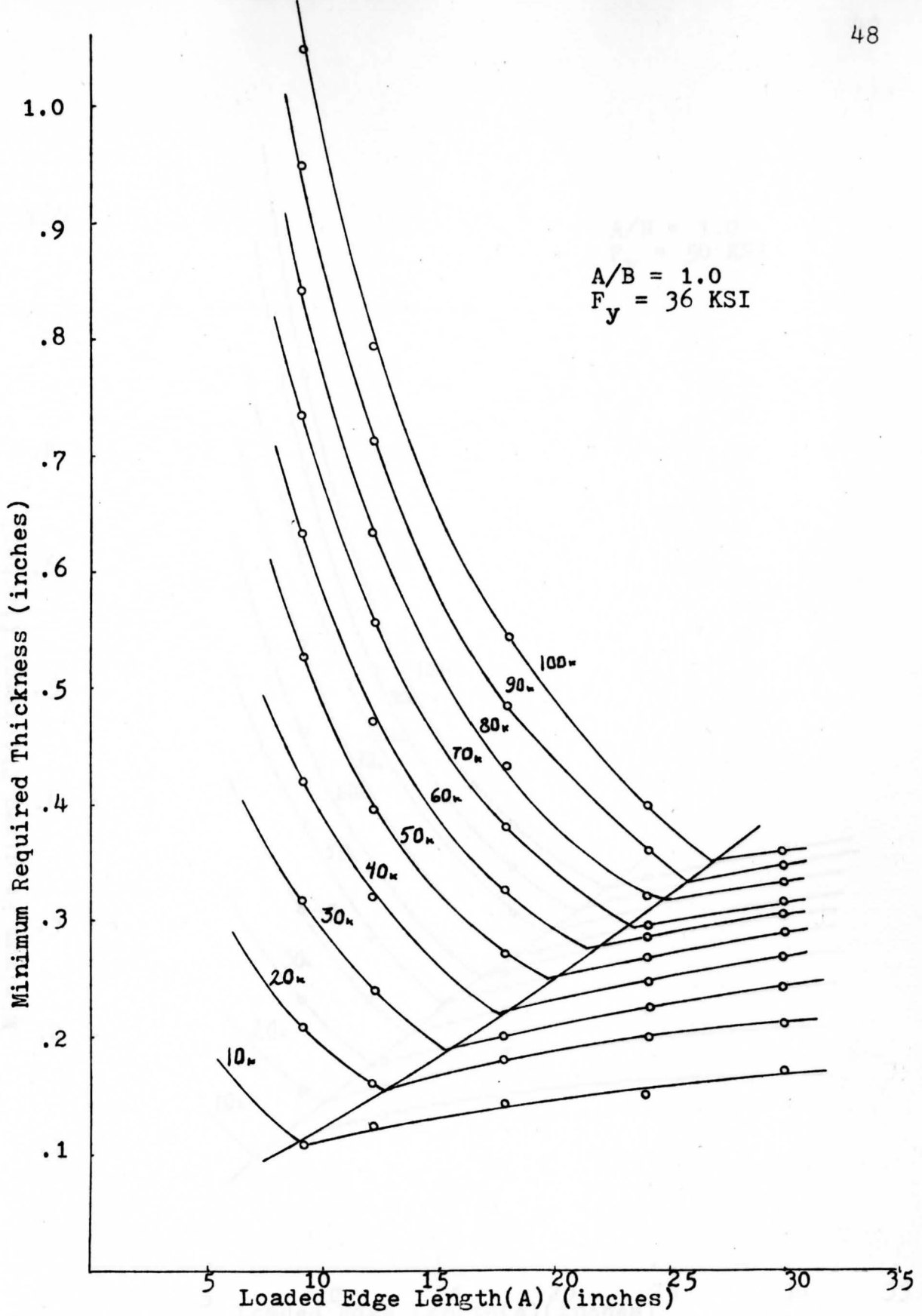


Fig. 3.14. Design Chart: Combined Criteria

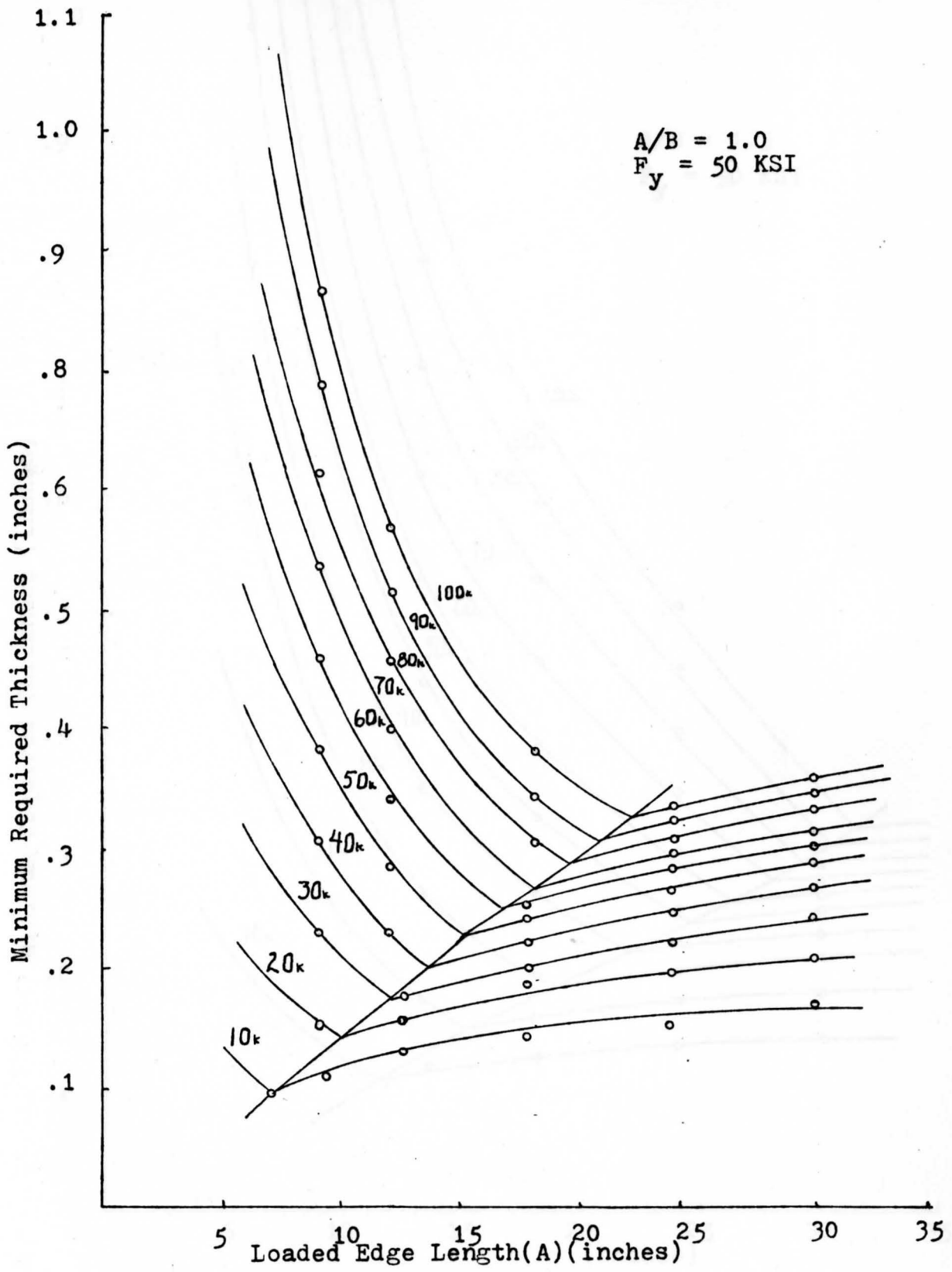


Fig. 3.15. Design Chart: Combined Criteria

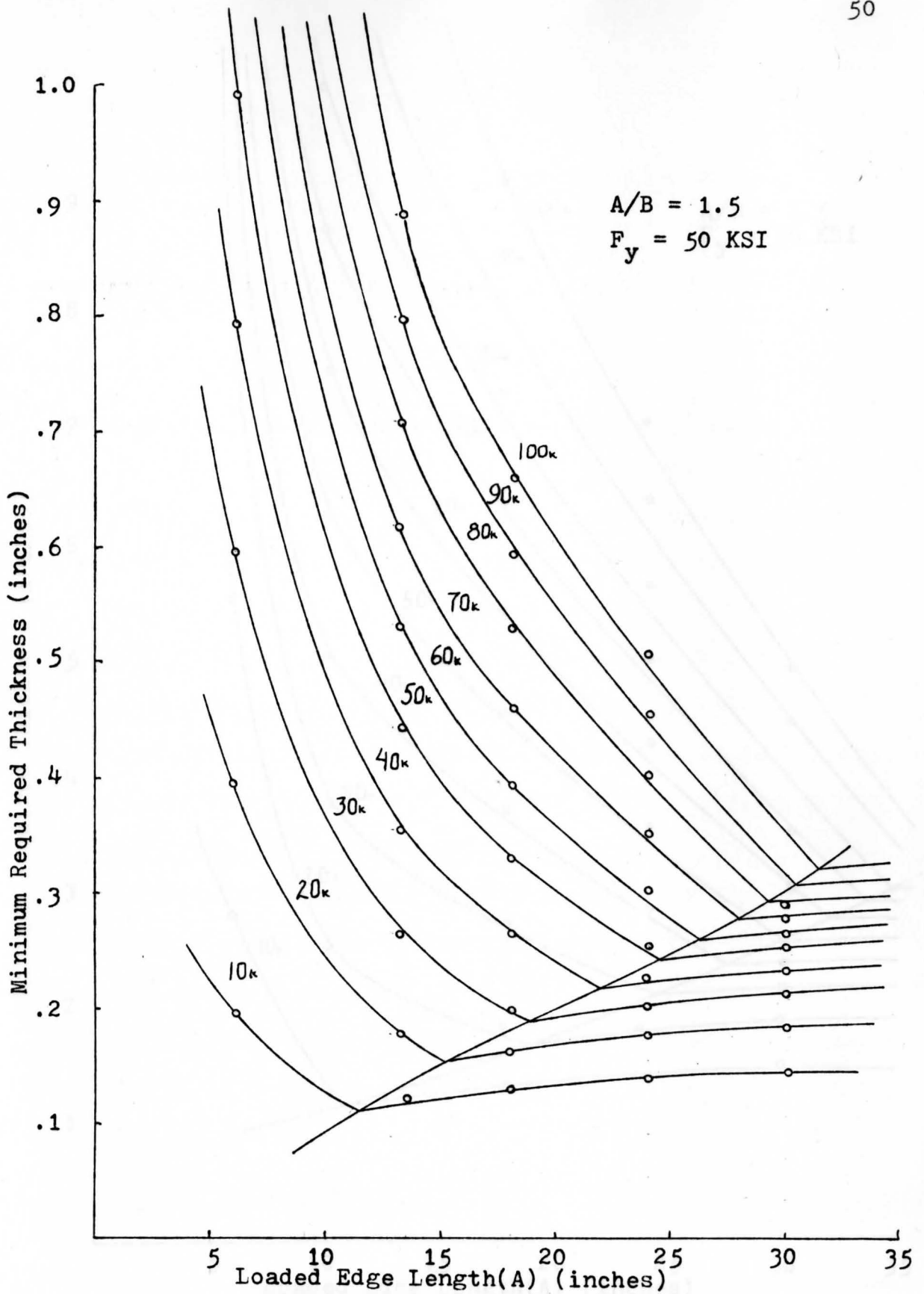


Fig. 3.16. Design Chart: Combined Criteria

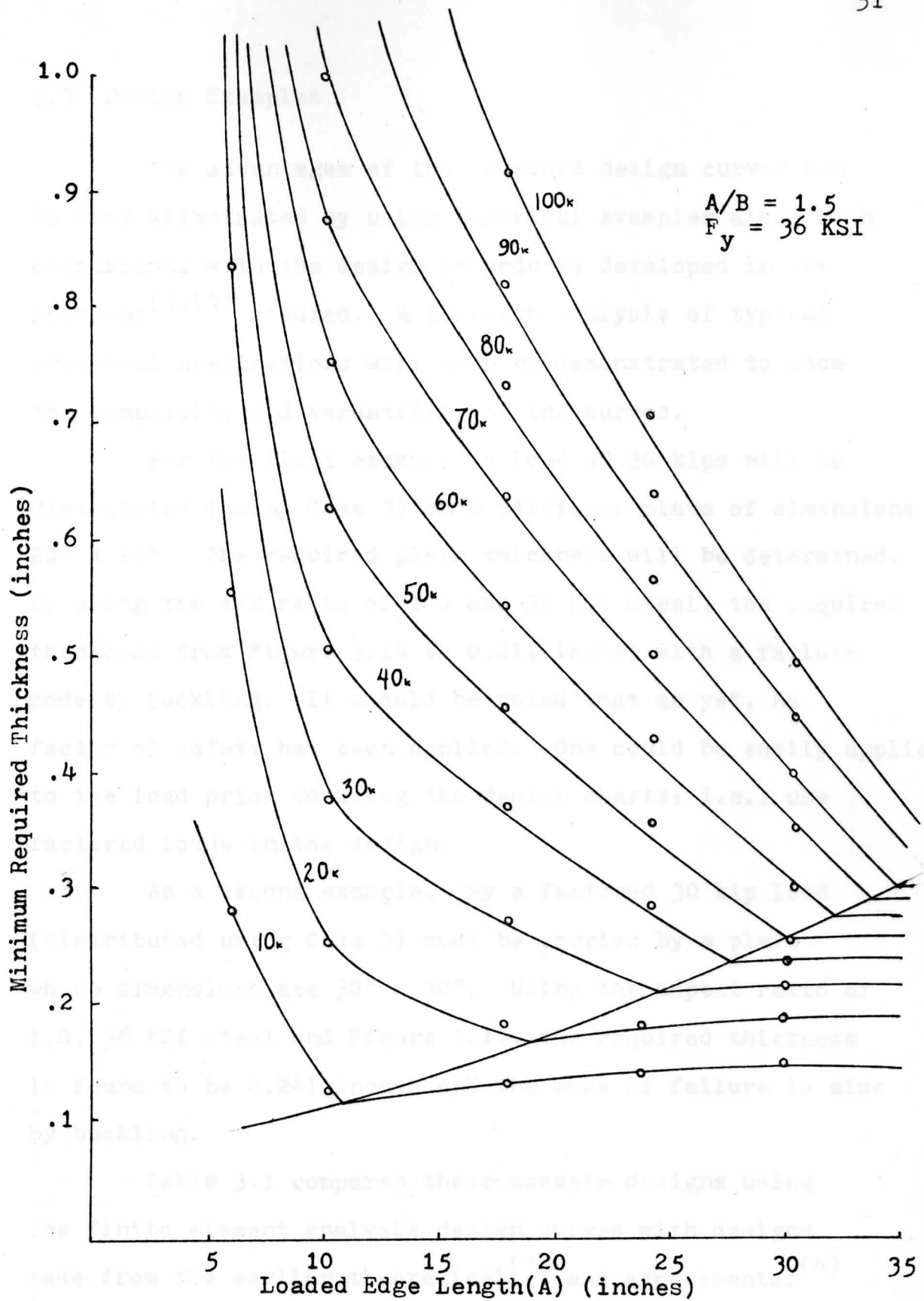


Fig. 3.17 Design Chart: Combined Criteria

3.3 Design Examples

The advantages of the proposed design curves can be best illustrated by using numerical examples along with comparisons with the design procedures developed in the previous⁽³⁾⁽⁴⁾ studies. A thorough analysis of typical practical applications will then be demonstrated to show the simplicity and versatility of the curves.

For the first example, a load of 30 kips will be distributed (using Case 3) on a stiffener plate of dimensions 20" x 20". The required plate thickness will be determined. By using the A/B ratio of 1.0 and 36 KSI steel, the required thickness from Figure 3.14 is 0.211 inches with a failure mode by buckling. It should be noted that as yet, no factor of safety has been applied. One could be easily applied to the load prior to using the design charts; i.e., use factored loads in the design.

As a second example, say a factored 30 kip load (distributed using Case 3) must be carried by a plate whose dimensions are 30" x 30". Using the aspect ratio of 1.0, 36 KSI steel and Figure 3.14, the required thickness is found to be 0.241 inches and the mode of failure is also by buckling.

Table 3.1 compares these example designs using the finite element analysis design curves with designs made from the earlier theoretical⁽³⁾ and experimental⁽⁴⁾ recommended procedures.

TABLE 3.1

DESIGN SPECIFICATION COMPARISON
THICKNESS AND FAILURE MODE

	Finite Element (inches)	Experimental (inches)	Salmon (inches)
Example 1	0.211 buckle-mode	0.231 buckle-mode	0.250 buckle-mode
Example 2	0.241 buckle-mode	0.254 buckle-mode	0.313 buckle-mode

These two numerical example designs were specifically chosen since the plate dimensions A & B were the same as those used in both the earlier theoretical and experimental studies. These dimensions were deliberately chosen on the large size to insure a buckling failure, particularly in the experimental procedure. Thus, these numerical examples served as a verification of the finite element procedure and they are not intended to serve as practical examples. In practice, the plate dimensions A & B are considerably less than 20" x 20" and 30" x 30" used in the verification examples. The following numerical example is intended to demonstrate a practical application of the developed design charts.

Suppose a W 18 x 45 requires a bearing length (n) of 9.0 inches to safely transmit a factored shear load of

90 kips to a connecting column. The aspect ratio can be dictated by several considerations to include architectural limitations, aesthetic factors, length and size of the connecting weld, etc. In this instance, the aspect ratio will be initially taken at 1.0. The steel will be taken as A36 grade and the loaded edge length(A) will be initially taken equal to the required bearing length of 9.0 inches. By using the design curves in Figure 3.14,,the minimum required thickness is 0.95 inches with failure controlled by yielding criteria. However, with the design curves available, other aspect ratios may be easily selected in order to optimize the volume and hence, the weight of the stiffener plate. Table 3.2 summarizes the trial designs for other aspect ratios and their respective volumes.

TABLE 3.2

COMPARATIVE DESIGN SUMMARY

Aspect Ratio	Thickness (inches)	Volume (inches ³)	Failure Mode	E60 Electrode & A36 Fillet Weld Size ($W_{max} = t/2$) (inches)
0.5	0.477 (1/2)*	38.63	yield	1/4
0.75	0.685 (11/16)	36.99	yield	5/16
1.0	0.95 (1)	38.48	yield	1/2
1.5	1.63 (1 5/8)	44.01	yield	13/16

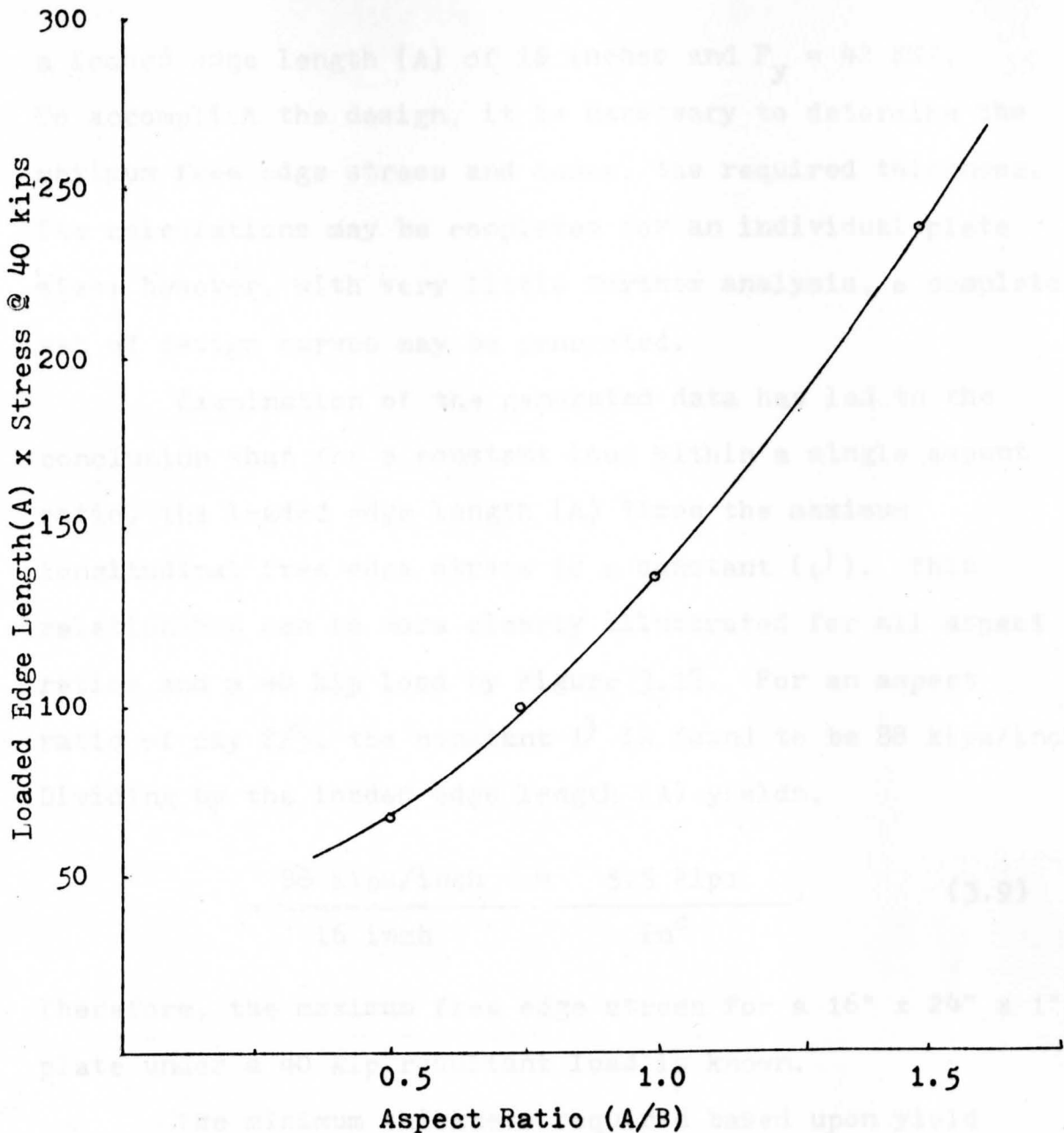
* Values rounded up to nearest standard size.

The weight was found to be minimum using an aspect ratio of 0.75, which is a weight reduction of 3.87% over the initial choice of 1.0.

Final selection of a plate thickness is also contingent upon the welding requirements. For example, the minimum fillet weld size for structural purposes is $3/16$ ". Thus, with a fillet weld on both sides of the supported edge, a minimum plate thickness of $3/8$ " is required to insure that a weld stronger than the base material is not applied. Also, the maximum fillet weld size that can be placed with a single pass ($5/16$ ") must also be considered for construction cost purposes. These considerations must be made in selecting the connecting or supporting length B. Typical fillet weld requirements are also shown on Table 3.2 for each design.

3.4 Mathematical Formulations

The aspect ratios analyzed in this study were thought to be the more commonly used ratios. It may become necessary, however, to have a set of design curves for an aspect ratio other than those selected. There are mathematical relationships evident which may be used to generate a set of design curves for any aspect ratio and yield stress. These relationships may be best developed by use of a numerical example. Say, for example, that the minimum thickness is required for a steel plate with an aspect ratio of $2/3$, a resultant applied load of 40 kips,



Thickness = one(1) inch
 Load = 40 kips

Fig. 3.18. Stress-Aspect Ratio Relationship

a loaded edge length (A) of 16 inches and $F_y = 42$ KSI. To accomplish the design, it is necessary to determine the maximum free edge stress and hence, the required thickness. The calculations may be completed for an individual plate size; however, with very little further analysis, a complete set of design curves may be generated.

Examination of the generated data has led to the conclusion that for a constant load within a single aspect ratio, the loaded edge length (A) times the maximum longitudinal free edge stress is a constant (\mathcal{D}). This relationship can be more clearly illustrated for all aspect ratios and a 40 kip load by Figure 3.18. For an aspect ratio of say 2/3, the constant \mathcal{D} is found to be 88 kips/inch. Dividing by the loaded edge length (A) yields,

$$\frac{88 \text{ kips/inch}}{16 \text{ inch}} = \frac{5.5 \text{ kips}}{\text{in}^2}. \quad (3.9)$$

Therefore, the maximum free edge stress for a 16" x 24" x 1" plate under a 40 kip resultant load is known.

The minimum thickness required based upon yield criteria is:

$$\frac{55 \text{ kips in in}^2}{\text{in}^2 42 \text{ kips}} = 0.131 \text{ inches}. \quad (3.10)$$

However, the minimum thickness to prevent premature buckling failure may be greater and must therefore be calculated.

By using equation (3.8), and a stiffness coefficient

$K = 100,000$ KSI (See Figure 1.3),

$$t_{\text{critical}} = \sqrt[3]{\frac{(5.15)(16)^2}{100,000}} \quad (3.11)$$

and,

$$t_{\text{critical}} = 0.241 \text{ inches.} \quad (3.12)$$

The minimum thickness required is the larger of the two values, or 0.241 inches with failure by buckling.

A complete set of design curves may be similarly generated.

3.5 Design Recommendations

The design curves developed by this study are primarily applicable to welded construction as illustrated in Figure 3.19. A factor of safety, when chosen with a sound

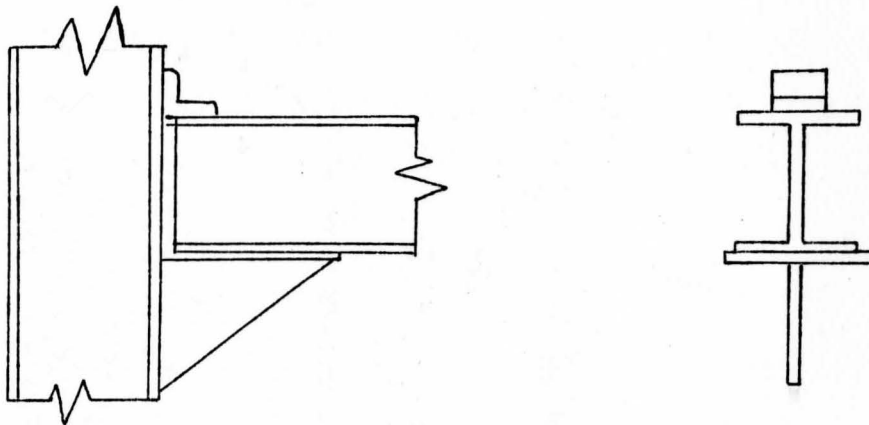


Fig. 3.19. Applicable Construction

engineering judgement, may be used as a load factor due to the nonuniformity of the curves. It must be noted, however, that welded constructions utilizes a minimum weld size of $3/16$ " and, in this case with welds on both sides as in Figure 3.19, a minimum plate thickness of $3/8$ "⁽⁷⁾; i.e., the welds cannot be such so as to exceed the capacity of the supported section or member.

- - - - -

CHAPTER 4

CONCLUSIONS

The capability of the finite element method of analysis to accurately model the stress distribution within the triangular plate problem using only the basic constant strain triangular element has been demonstrated by this study. However, irregardless of the sophistication of analysis technique, both supplemental theoretical and experimental verifications must be performed in order to determine the correct model configuration, loading distribution and boundary conditions. Without these supplemental verifications, especially the experimental portion, the finite element analysis will be weak and unreliable. Thus, in this study heavy reliance was placed on the previous investigations. Through this approach, analysis with constant verification checks, design curves were developed and shown to closely approximate the design specifications set forth by the previous investigators and designers.

The real advantage in applying the design curves lies in the large scale design and fabrication of pre-engineered steel buildings. Here design with either hot or cold rolled sections allows for optimization (by minimum weight and weld size) of structural elements such as triangular stiffener plates with possible resultant

savings multiplied over many hundreds of repetitious buildings.

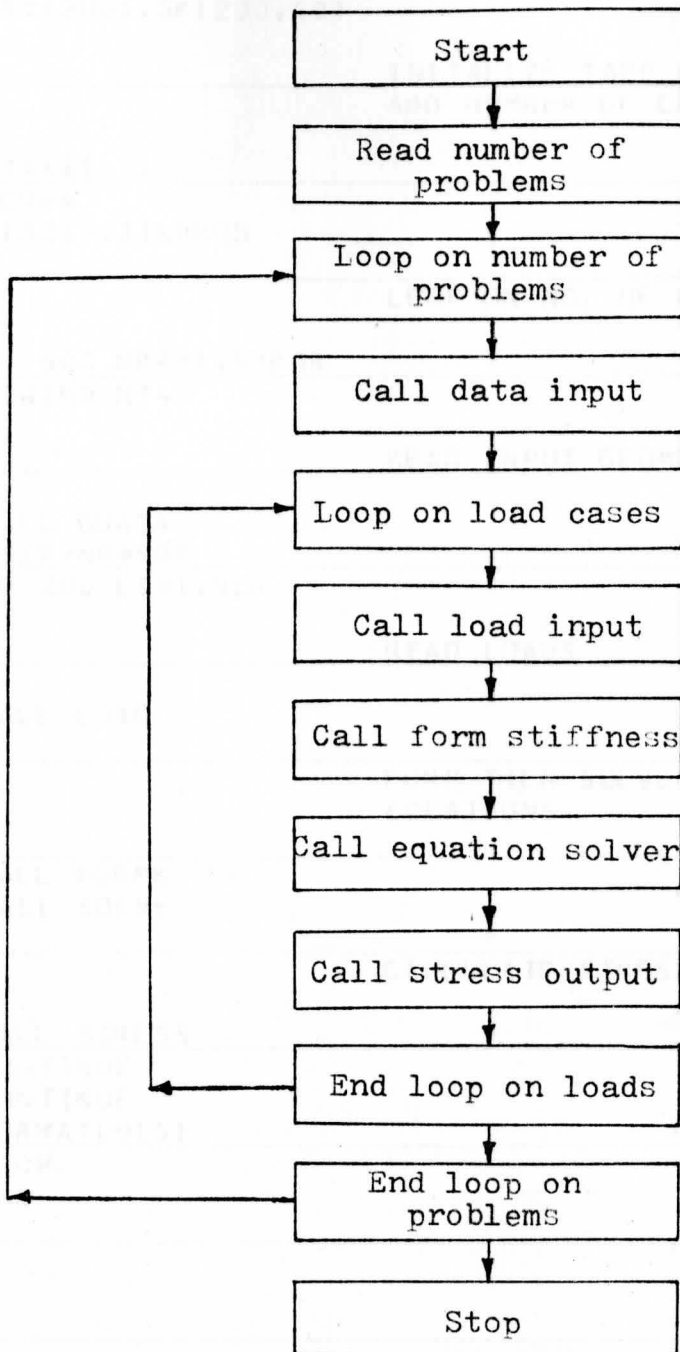
Further investigation, both theoretical and experimental, of the triangular beam seat stiffener plate is recommended. A finite element analysis with a more sophisticated basic element(s), including plate elements, and configurations with more elements would be desirable. In-plane displacements of the nodes could be incorporated into such an analysis to perhaps verify the buckling configuration used in the previous analytical studies.

APPENDIX A

The finite element program developed by Zienkiewicz-Cheung⁽²⁾, which was used in this study, is listed here along with flow charts. The program consists of a main program plus six(6) subroutines to accomplish the analysis. The flow charts, the program documentation, plus an example, are sufficient for an understanding of the program.



CONTROL
MAIN
PROGRAM



CONTROL
MAIN
PROGRAM

```
C CONTROL MAIN PROGRAM
COMMON/CONTR/TITLE(18),NP,NE,NB,NDF,NCN,NLD,NMAT,NSZF,LI,NT4
COMMON CORD(100,2),NOP(200,4),IMAT(200),ORT(25,2),NBC(25),NFIX(25
1,R1(200),SK(200,40)

C
C INITIALIZE TAPE NO.
C ADD NUMBER OF CORNER NODE MAX.
C
NT4=11
NCN=4
READ(5,1)NPROB

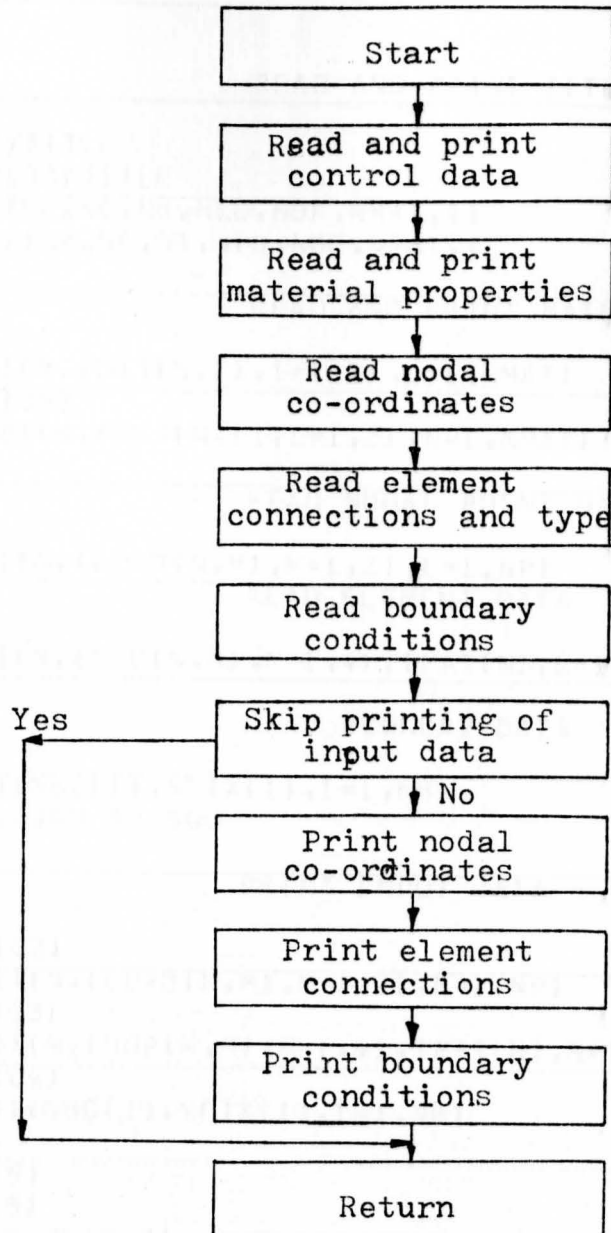
C
C LOOP ON NO. OF PROBLEMS
C
DO 400 NPR=1,NPROB
REWIND NT4

C
C READ INPUT GEOMETRY AND PROP.
C
CALL GDATA
NSZF=NP*NDF
DO 200 LI=1,NLD

C
C READ LOADS
C
CALL LOAD

C
C FORM THEN SOLVE SIMULTANEOUS
C EQUATIONS
C
CALL FORMK
CALL SOLVE

C
C CALCULATE STRESSES
C
CALL STRESS
200 CONTINUE
400 CONTINUE
1 FORMAT(9I5)
STOP
END
```



subroutine
GDATA

SUBROUTINE GDATA

COMMON/CONTR/TITLE(18),NP,NE,NB,NDF,NCN,NLD,NMAT,NSZF,LI,NT4
 COMMON CORD(100,2),NOP(200,4),IMAT(200),ORT(25,2),NBC(25),NFI(25)
 1,P1(200),SK(200,40)
 2,R(3)

C
 C READ AND PRINT TITLE AND CONTROL
 C

READ(5,7)TITLE
 WRITE(6,100)TITLE
 READ(5,1)NP,NE,NB,NLD,NDF,NMAT,I1
 WRITE(6,1)NP,NE,NB,NLD,NDF,NMAT,I1

C
 C READ AND PRINT MATERIAL DATA
 C

READ(5,8)(N,(ORT(N,I),I=1,2),L=1,NMAT)
 WRITE(6,108)
 WRITE(6,8)(N,(ORT(N,I),I=1,2),N=1,NMAT)

C
 C READ NODAL POINT DATA
 C

READ(5,2)(N,(CORD(N,M),M=1,2),L=1,NP)

C READ ELEMENT DATA

C
 READ(5,3)(N,(NOP(N,M),M=1,4),IMAT(N),L=1,NE)

C
 C READ BOUNDARY DATA
 C

READ(5,4)(NBC(I),NFI(I),I=1,NB)
 480 IF(I1.NE.0)GO TO 500

C
 C PRINT INPUT DATA
 C

WRITE(6,102)
 WRITE(6,2)(N,(CORD(N,M),M=1,2),N=1,NP)
 WRITE(6,103)
 WRITE(6,3)(N,(NOP(N,M),M=1,4),IMAT(N),N=1,NE)
 WRITE(6,104)
 WRITE(6,4)(NBC(I),NFI(I),I=1,NB)

500 CONTINUE

1 FORMAT(9I5)

3 FORMAT(6I5)

2 FORMAT(I10,2F10.3)

4 FORMAT(2I5)

7 FORMAT(18A4)

8 FORMAT(I10,2F10.2)

100 FORMAT(1H1,18A4)

102 FORMAT(20H0 NODAL POINTS)

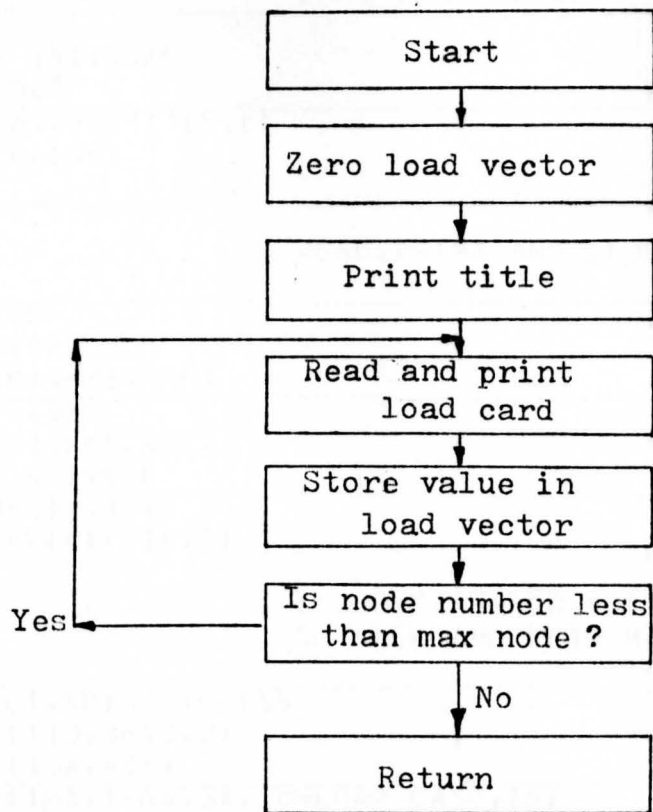
103 FORMAT(20H0 ELEMENTS)

104 FORMAT(21H0 BOUNDARY CONDITIONS)

108 FORMAT(1H0,20H MATERIAL PROPERTIES)

RETURN

END



subroutine
LOAD

SUBROUTINE LOAD

```
COMMON/CONTR/TITLE(18),NP,NE,NB,NDF,NCN,NLD,NMAT,NSZF,LI,NT4
COMMON CORD(100,2),NOP(200,4),IMAT(200),ORT(25,2),NBC(25),NFI(25)
1,R1(200),SK(200,40)
2,R(3)
```

C
C
C

ZERO LOAD ARRAY

```
DO 160 J=1,NSZF
160 R1(J)=0.0
WRITE(6,100)TITLE,LI
WRITE(6,109)
```

C
C
C
C

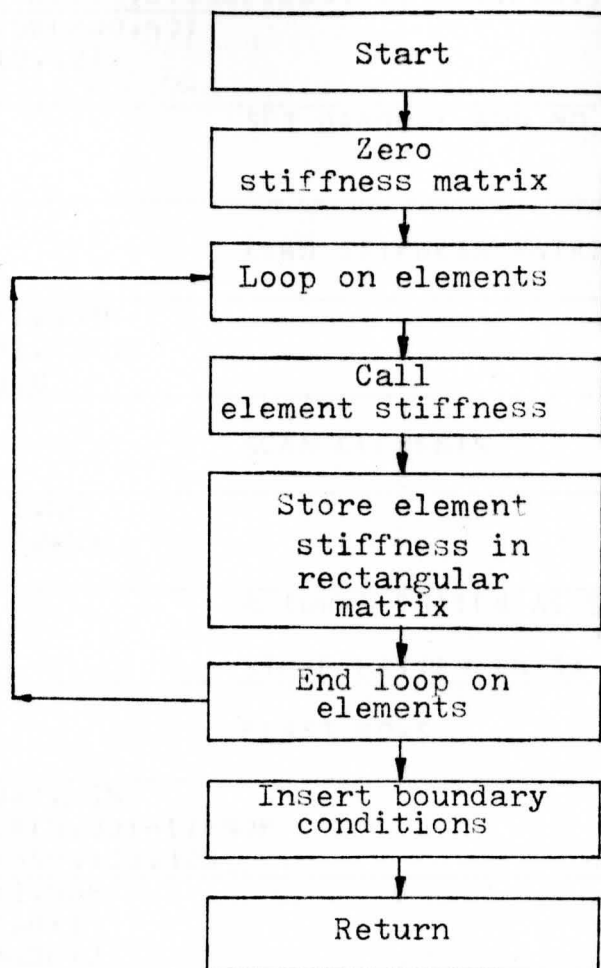
READ, PRINT AND STORE LOAD CARD

```
165 CONTINUE
READ(5,9)
INQ,(R(K),K=1,NDF)
WRITE(6,9)
INQ,(R(K),K=1,NDF)
DO 170 K=1,NDF
IC=(NQ-1)*NDF+K
170 R1(IC)=R(K)+R1(IC)
```

C
C
C
C

IF NODE NUMBER NOT MAX. NODE PT.
GO BACK AND READ MORE

```
IF(NQ.LT.NP)GO TO 165
9 FORMAT(110,3F10.2)
20 FORMAT(10X,4I5)
100 FORMAT(1H1,18A4,5X,10HLOAD CASE,15)
109 FORMAT(1H0,6H LOADS)
RETURN
END
```



subroutine
FORMK

SUBROUTINE FORMK

FORMS STIFFNESS MATRIX
IN UPPER TRIANGULAR FORM

COMMON/CONTR/TITLE(18),NP,NE,NB,NDF,NCN,NLD,NMAT,NSZF,LI,NT4
COMMON CORD(100,2),NDP(200,4),IMAT(200),ORT(25,2),NBC(25),NFI(25)
1,R1(200),SK(200,40)
2,ESTIFM(12,12)

SET BANDMAX AND NO OF EQUATIONS

NBAND=40

ZERO STIFFNESS MATRIX

DO 300 N=1,NSZF
DO 300 M=1,NBAND
300 SK(N,M)=0.0

SCAN ELEMENTS

DO 400 N=1,NE
CALL STIFT2(N)

RETURNS ESTIFM AS STIFFNESS MATRIX

STORE ESTIFM IN SK

FIRST ROWS

DO 350 JJ=1,NCN
NRDWB=(NDP(N,JJ)-1)*NDF
IF(NRDWB)350,305,305
305 DO 350 J=1,NDF
NRDWB=NRDWB+1
I=(JJ-1)*NDF+J

THEN COLUMNS

DO 330 KK=1,NCN
NCOLB=(NDP(N,KK)-1)*NDF
DO 320 K=1,NDF
L=(KK-1)*NDF+K
NCOL=NCOLB+K+1-NRDWB

SKIP STORING IF BELOW BAND

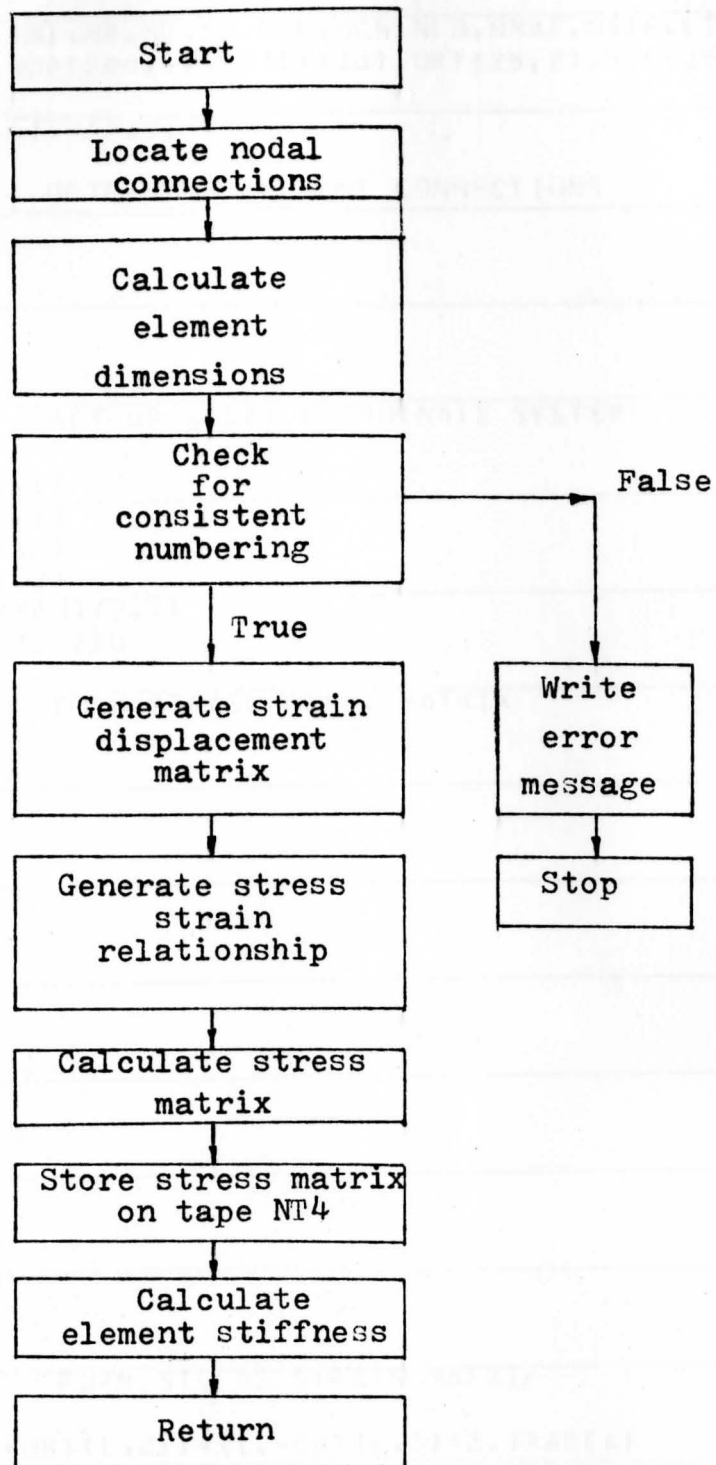
IF(NCOL)320,320,310
310 SK(NRDWB,NCOL)=SK(NRDWB,NCOL)+ESTIFM(I,L)
320 CONTINUE
330 CONTINUE
350 CONTINUE
400 CONTINUE

INSERT BOUNDARY CONDITIONS

```
C
C
DO 500 N=1,NB
NX=10** (NDF-1)
I=NBC(N)
NROWB=(I-1)*NDF
```

EXAMINE EACH DEGREE OF FREEDOM

```
C
C
DO 490 M=1,NDF
NROWB=NROWB+1
ICON=NFIX(N)/NX
IF (ICON) 450,450,420
420 SK(NROWB,1)=1.0
DO 430 J=2,NBAND
SK(NROWB,J)=0.0
NR=NROWB+1-J
IF (NR) 430,430,425
425 SK(NR,J)=0.0
430 CONTINUE
NFIX(N)=NFIX(N)-NX*ICON
450 NX=NX/10
490 CONTINUE
500 CONTINUE
RETURN
END
```



subroutine
STIFT2

SUBROUTINE STIFT2(N)

```
COMMON/CONTR/TITLE(18),NP,NE,NB,NDF,NCN,NLD,NMAT,NSZF,LI,NT4
COMMON CORD(100,2),NOP(200,4),IMAT(200),ORT(25,2),NBC(25),NFI(25)
1,R1(200),SK(200,4)
2,ESTIFM(12,12),A(3,6),B(3,9)
```

```
C
C
C          DETERMINE ELEMENT CONNECTIONS
```

```
I=NOP(N,1)
J=NOP(N,2)
K=NOP(N,3)
L=IMAT(N)
```

```
C
C          SET UP LOCAL COORDINATE SYSTEM
```

```
AJ=CORD(J,1)-CORD(I,1)
AK=CORD(K,1)-CORD(I,1)
BJ=CORD(J,2)-CORD(I,2)
BK=CORD(K,2)-CORD(I,2)
AREA=ABS(((AJ*BK-AK*BJ)/2.))
IF(AREA .LE. 0.)GO TO 220
```

```
C
C          FORM STRAIN DISP. MATRIX
```

```
A(1,1)=BJ-BK
A(1,2)=0.0
A(1,3)=BK
A(1,4)=0.0
A(1,5)=-BJ
A(1,6)=0.0
A(2,1)=0.0
A(2,2)=AK-AJ
A(2,3)=0.0
A(2,4)=-AK
A(2,5)=0.0
A(2,6)=AJ
A(3,1)=AK-AJ
A(3,2)=BJ-BK
A(3,3)=-AK
A(3,4)=BK
A(3,5)=AJ
A(3,6)=-BJ
```

```
C
C          FORM STRESS STRAIN MATRIX
```

```
COMM=ORT(L,1)/((1.+ORT(L,2))*(1.-ORT(L,2)*2.)*AREA)
ESTIFM(1,1)=COMM*(1.-ORT(L,2))
ESTIFM(1,2)=COMM*ORT(L,2)
ESTIFM(1,3)=0.0
ESTIFM(2,1)=ESTIFM(1,2)
ESTIFM(2,2)=ESTIFM(1,1)
ESTIFM(2,3)=0.0
ESTIFM(3,1)=0.0
ESTIFM(3,2)=0.0
ESTIFM(3,3)=ORT(L,1)/(2.*(1.+ORT(L,2))*AREA)
```

C
C B IS THE STRESS BACKSUBSTITUTION
C MATRIX AND IS SAVED ON TAPE
C

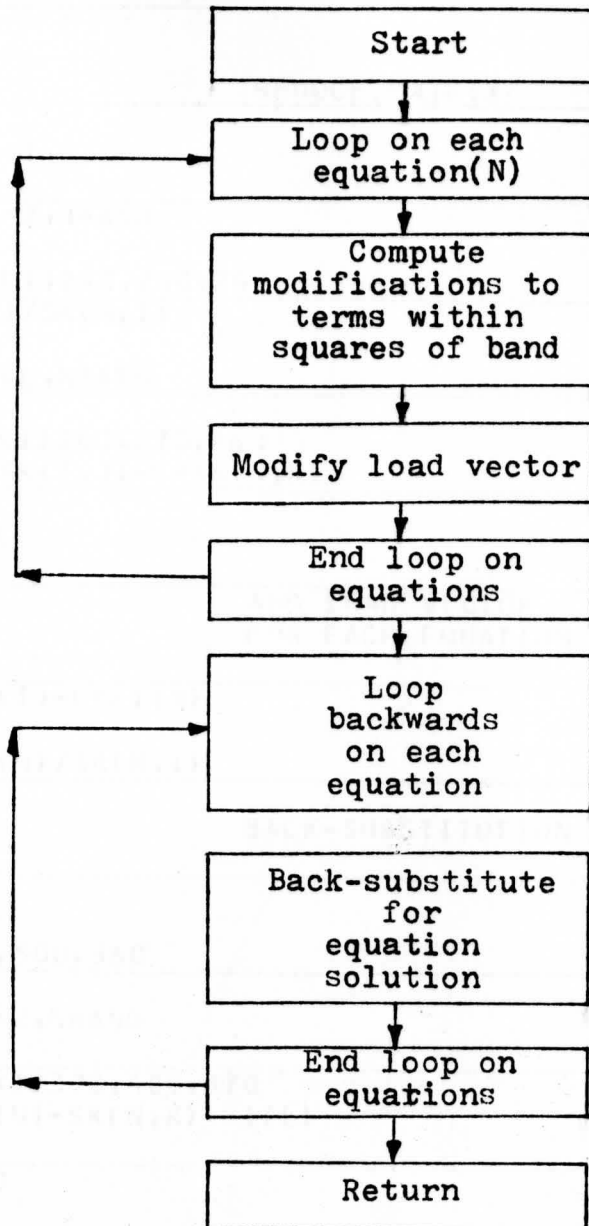
```
DD 205 I=1,3
DD 205 J=1,6
B(I,J)=0.0
DD 205 K=1,3
205 B(I,J)=B(I,J)+ESTIFM(I,K)/2.*A(K,J)
WRITE(NT4)N,((B(I,J),J=1,6),I=1,3)
```

C
C ESTIFM IS STIFNESS MATRIX
C

```
DD 210 I=1,6
DD 210 J=1,6
ESTIFM(I,J)=0.0
DD 210 K=1,3
210 ESTIFM(I,J)=ESTIFM(I,J)+B(K,I)/2.*A(K,J)
RETURN
```

C
C ERROR EXIT FOR BAD CONNECTIONS
C

```
220 WRITE(6,100)N
100 FORMAT(33HZERO OR NEGATIVE AREA ELEMENT NOI4/21HOEXECUTION TERMIN
LATED)
STOP
END
```



subroutine
SOLVE

SUBROUTINE SOLVE

C
C
C

SPECIFICATION STATEMENTS

```
COMMON/CONTR/TITLE(18),NP,NE,NB,NDF,NCN,NLD,NMAT,NSZF,LI,NT4
COMMON CORD(100,2),NDP(200,4),IMAT(200),ORT(25,2),NBC(25),NFIX(25)
I,R1(200),SK(200,40)
NBAND=40
```

C
C
C

REDUCE MATRIX

```
DO 300 N=1,NSZF
  T=N
  DO 290 L=2,NBAND
    I=I+1
    IF(SK(N,L))240,290,240
240 C=SK(N,L)/SK(N,1)
    J=0
    DO 270 K=L,NBAND
      J=J+1
      IF(SK(N,K))260,270,260
260 SK(I,J)=SK(I,J)-C*SK(N,K)
270 CONTINUE
280 SK(N,L)=C
```

C
C
C
CAND LOAD VECTOR
FOR EACH EQUATION

```
R1(I)=R1(I)-C*R1(N)
290 CONTINUE
300 R1(N)=R1(N)/SK(N,1)
```

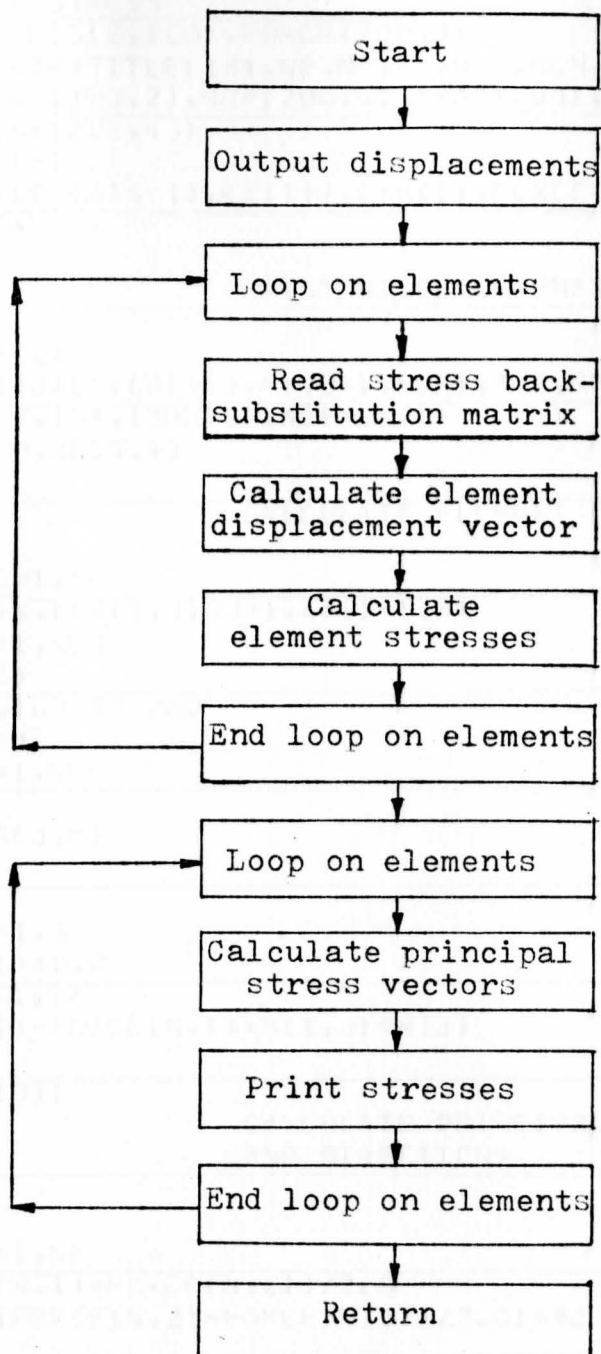
C
C
C

BACK-SUBSTITUTION

```
N=NSZF
350 N=N-1
  IF(N)500,500,360
360 L=N
  DO 400 K=2,NBAND
    L=L+1
    IF(SK(N,K))370,400,370
370 R1(N)=R1(N)-SK(N,K)*R1(L)
400 CONTINUE
  GO TO 350
```

C

```
500 RETURN
  END
```



subroutine
STRESS

SUBROUTINE STRESS

```

DIMENSION DIS(2,100),FORCE(200,3)
COMMON/CONTR/TITLE(18),NP,NE,NB,NDF,NCN,NLD,NMAT,NSZF,LI,NT4
COMMON CORD(100,2),NOP(200,4),IMAT(200),ORT(25,2),NBC(25),NFIX(25)
1,R1(200),SK(200,40)
2,B(3,6),R(8)
EQUIVALENCE (DIS(1),R1(1)),(SK(1),FORCE(1))
REWIND NT4

```

```

C
C
C          PRINT DISPLACEMENTS

```

```

WRITE(6,100)
WRITE(6,110)(M,(DIS(J,M),J=1,NDF),M=1,NP)
100 FORMAT(///,15X,13HDISPLACEMENTS      )
110 FORMAT(I10,2F15.4)

```

```

C
C
C          CALCULATE ELEMENT FORCES

```

```

DO 200 NC=1,NE
READ(NT4)N,((B(I,J),J=1,6),I=1,3)
DO 260 I=1,NCN
M=NOP(N,I)
IF(M.EQ.0)GO TO 260
K=(I-1)*NDF
DO 240 J=1,NDF
IJ=J+K
240 R(IJ)=DIS(J,M)
260 CONTINUE
IA=K+NDF
DO 300 I=1,3
FORCE(N,I)=0.0
DO 300 J=1,IA
300 FORCE(N,I)=FORCE(N,I)+B(I,J)*R(J)
200 CONTINUE
WRITE(6,101)

```

```

C
C
C          CALCULATE PRINCIPAL STRESSES
AND DIRECTIONS

```

```

DO 600 N=1,NE
250 C=(FORCE(N,1)+FORCE(N,2))/2.0
A=SQRT(((FORCE(N,2)-FORCE(N,1))/2.0)**2 +FORCE(N,3)**2)
SMAX=C+A
SMIN=C-A
IF(FORCE(N,2).EQ.SMIN)GO TO 700
ANG=57.29578*ATAN(FORCE(N,3)/(FORCE(N,2)-SMIN))
GO TO 210
700 ANG=90.0
210 CONTINUE

```

```

C
C
C          WRITE ALL STRESS COMPONENTS

```

```

400 WRITE(6,111)
1N,(FORCE(N,I),I=1,3),SMAX,SMIN,ANG
600 CONTINUE

```



```

101 FORMAT(107H0      ELEMENT      X-STRESS      Y-STRESS      XY
1-STRESS      MAX-STRESS      MIN-STRESS      ANGLE      )
111 FORMAT(110,5F17.4,F12.3)
RETURN
END

```

1.1) Title Card (12X6)

1.2) Input Card (12X6)

1.3) Output Card (12X6)

1.4) Material Cards (110,25F10.0) 1 for each material:

Card Range	Field	Description	Format
1-10*	1-10*	Material Number	(N)
11-20	11-20	Young's modulus	(GPR(3,1))
21-30	21-30	Poisson's ratio	(GPR(4,1))

1.5) Coordinate Cards (110,25F10.0) 1 for each node point

Card Range	Field	Description	Format
1-10*	1-10*	Node Number	(N)
11-20	11-20	X-Coordinate	(COORD(X,1))
21-30	21-30	Y-Coordinate	(COORD(X,2))

1.6) Element Cards (115) 1 for each element

Card Range	Field	Description	Format
1-5*	1-5*	Element Number	(N)
6-10*	6-10*	1	(NCP(N,1))
11-15*	11-15*	2	(NCP(N,2))
16-20*	16-20*	3	(NCP(N,3))
21-25	21-25	not used	(NCP(N,4))
26-30*	26-30*	Material number	(MAT(N))

1.7) Boundary Cards (215) 1 for each boundary condition

Card Range	Field	Description	Format
1-5*	1-5*	Boundary node number	(BN(1))
6-10*	6-10*	01 Fixed in Y direction	
		10 Fixed in X direction	
		11 Fixed in both directions	(BN(2))

*Indicates that numbers should be right adjusted with no decimal point in the field, all other numbers should have decimal points ignored.

8.) Load Cards (I10,2F10.2) 1 for each loaded point

Col 1-10*	Node number	NQ
11-20	X-Load	R(1)
21-30	Y-Load	R(2)

Note: Load cards are terminated with a load at the last numbered node whether or not a load exists there.

For an example, a 23" x 24" x 1" plate is loaded with a 40 kip load in Configuration 3 (See Figure 2.3). Young's modulus is taken as 29,500,000 psi and ν as 0.295. Figure A.1 illustrates the problem. The computer results follow.

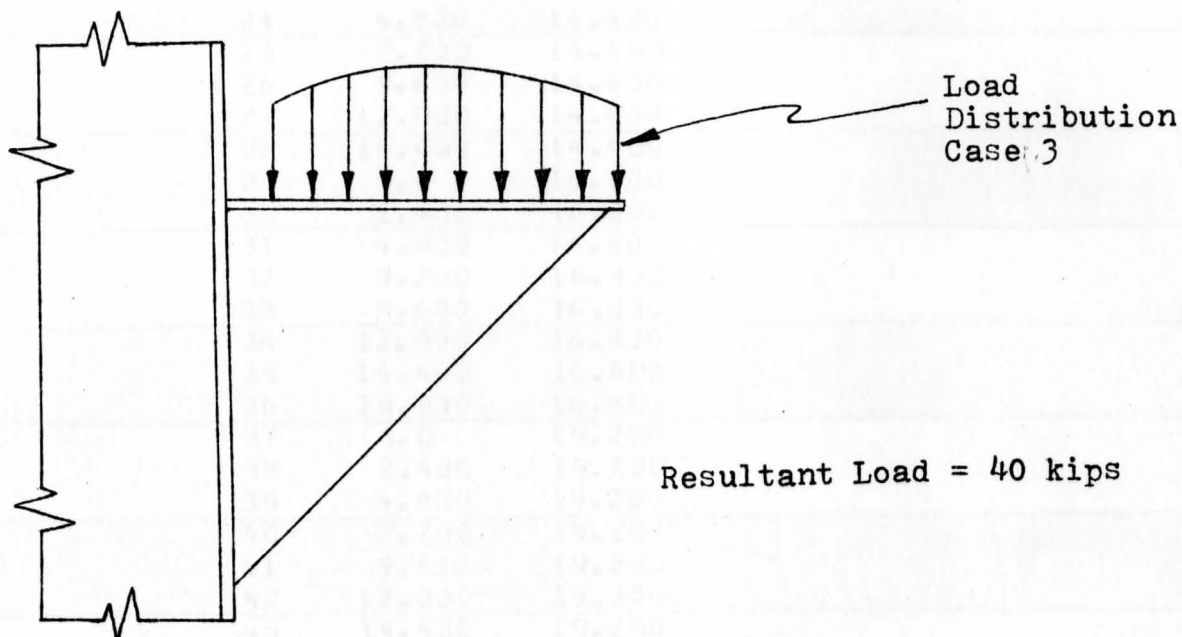


Fig. A.1. Sample problem (24" x 24" x 1")

1 TRIANGULAR PLATE, A=B=24.

66 100 21 1 2 1 0

0 MATERIAL PROPERTIES

1 29500.00 0.30

0 NODAL POINTS

1	0.0	0.0
2	0.0	2.400
3	2.400	2.400
4	0.0	4.800
5	2.400	4.800
6	4.800	4.800
7	0.0	7.200
8	2.400	7.200
9	4.800	7.200
10	7.200	7.200
11	0.0	9.600
12	2.400	9.600
13	4.800	9.600
14	7.200	9.600
15	9.600	9.600
16	0.0	12.000
17	2.400	12.000
18	4.800	12.000
19	7.200	12.000
20	9.600	12.000
21	12.000	12.000
22	0.0	14.400
23	2.400	14.400
24	4.800	14.400
25	7.200	14.400
26	9.600	14.400
27	12.000	14.400
28	14.400	14.400
29	0.0	16.800
30	2.400	16.800
31	4.800	16.800
32	7.200	16.800
33	9.600	16.800
34	12.000	16.800
35	14.400	16.800
36	16.800	16.800
37	0.0	19.200
38	2.400	19.200
39	4.800	19.200
40	7.200	19.200
41	9.600	19.200
42	12.000	19.200
43	14.400	19.200
44	16.800	19.200
45	19.200	19.200
46	0.0	21.600
47	2.400	21.600
48	4.800	21.600
49	7.200	21.600
50	9.600	21.600
51	12.000	21.600
52	14.400	21.600
53	16.800	21.600
54	19.200	21.600
55	21.600	21.600

59	7.200	24.000
60	9.600	24.000
61	12.000	24.000
62	14.400	24.000
63	16.800	24.000
64	19.200	24.000
65	21.600	24.000
66	24.000	24.000

0 ELEMENTS

1	1	2	3	0	1
2	2	5	4	0	1
3	2	3	5	0	1
4	3	6	5	0	1
5	4	8	7	0	1
6	5	4	8	0	1
7	5	9	8	0	1
8	5	6	9	0	1
9	6	10	9	0	1
10	7	12	11	0	1
11	7	8	12	0	1
12	8	13	12	0	1
13	8	9	13	0	1
14	9	14	13	0	1
15	9	10	14	0	1
16	10	15	14	0	1
17	11	17	16	0	1
18	11	12	17	0	1
19	12	18	17	0	1
20	12	13	18	0	1
21	13	19	18	0	1
22	13	14	19	0	1
23	14	20	19	0	1
24	14	15	20	0	1
25	15	21	20	0	1
26	16	23	22	0	1
27	16	17	23	0	1
28	17	24	23	0	1
29	17	18	24	0	1
30	18	25	24	0	1
31	18	19	25	0	1
32	19	26	25	0	1
33	19	20	26	0	1
34	20	27	26	0	1
35	20	21	27	0	1
36	21	28	27	0	1
37	22	30	29	0	1
38	22	23	30	0	1
39	23	31	30	0	1
40	23	24	31	0	1
41	24	32	31	0	1
42	24	25	32	0	1
43	25	33	32	0	1
44	25	26	33	0	1
45	26	34	33	0	1
46	26	27	34	0	1
47	27	35	34	0	1
48	27	28	35	0	1
49	28	36	35	0	1
50	29	38	37	0	1
51	29	30	38	0	1
52	30	39	38	0	1
53	30	31	39	0	1
54	31	40	39	0	1

58	33	42	41	0	1
59	33	34	42	0	1
60	34	43	42	0	1
61	34	35	43	0	1
62	35	44	43	0	1
63	35	36	44	0	1
64	36	45	44	0	1
65	37	47	46	0	1
66	37	38	47	0	1
67	38	48	47	0	1
68	38	39	48	0	1
69	39	49	48	0	1
70	39	40	49	0	1
71	40	50	49	0	1
72	40	41	50	0	1
73	41	51	50	0	1
74	41	42	51	0	1
75	42	52	51	0	1
76	42	43	52	0	1
77	43	53	52	0	1
78	43	44	53	0	1
79	44	54	53	0	1
80	44	45	54	0	1
81	45	55	54	0	1
82	46	57	56	0	1
83	46	47	57	0	1
84	47	58	57	0	1
85	47	48	58	0	1
86	48	59	58	0	1
87	48	49	59	0	1
88	49	60	59	0	1
89	49	50	60	0	1
90	50	61	60	0	1
91	50	51	61	0	1
92	51	62	61	0	1
93	51	52	62	0	1
94	52	63	62	0	1
95	52	53	63	0	1
96	53	64	63	0	1
97	53	54	64	0	1
98	53	65	64	0	1
99	54	55	65	0	1
100	55	66	65	0	1

0 BOUNDARY CONDITIONS

1	11
2	11
4	11
7	11
11	11
16	11
22	11
29	11
37	11
46	11
56	11
57	10
58	10
59	10
60	10
61	10
62	10
63	10
64	10

58	0.0	-1.60
59	0.0	-2.40
60	0.0	-3.20
61	0.0	-4.80
62	0.0	-6.40
63	0.0	-8.00
64	0.0	-6.40
65	0.0	-4.80
66	0.0	-2.40

DISPLACEMENTS

1	0.0	0.0
2	0.0	0.0
3	-0.0001	-0.0003
4	0.0	0.0
5	-0.0001	-0.0003
6	-0.0002	-0.0007
7	0.0	0.0
8	-0.0001	-0.0004
9	-0.0003	-0.0008
10	-0.0004	-0.0011
11	0.0	0.0
12	-0.0002	-0.0004
13	-0.0003	-0.0008
14	-0.0005	-0.0012
15	-0.0006	-0.0017
16	0.0	0.0
17	-0.0002	-0.0004
18	-0.0003	-0.0008
19	-0.0005	-0.0013
20	-0.0006	-0.0018
21	-0.0007	-0.0024
22	0.0	0.0
23	-0.0002	-0.0004
24	-0.0003	-0.0008
25	-0.0004	-0.0013
26	-0.0006	-0.0019
27	-0.0007	-0.0025
28	-0.0008	-0.0031
29	0.0	0.0
30	-0.0001	-0.0004
31	-0.0003	-0.0008
32	-0.0004	-0.0014
33	-0.0005	-0.0019
34	-0.0006	-0.0026
35	-0.0007	-0.0033
36	-0.0008	-0.0040
37	0.0	0.0
38	-0.0001	-0.0004
39	-0.0002	-0.0009
40	-0.0003	-0.0014
41	-0.0004	-0.0020
42	-0.0005	-0.0027
43	-0.0005	-0.0034
44	-0.0006	-0.0041
45	-0.0007	-0.0049
46	0.0	0.0
47	-0.0001	-0.0004
48	-0.0001	-0.0009
49	-0.0002	-0.0014

52	0.0003	-0.0033
53	-0.0003	-0.0043
54	-0.0003	-0.0050
55	-0.0004	-0.0059
56	0.0	0.0
57	0.0	-0.0004
58	0.0	-0.0009
59	0.0	-0.0015
60	0.0	-0.0021
61	0.0	-0.0029
62	0.0	-0.0037
63	0.0	-0.0045
64	0.0	-0.0052
65	0.0	-0.0060
66	0.0	-0.0069

ELEMENT	X-STRESS	Y-STRESS	XY-STRESS	MAX-STRESS	MIN-STRESS	ANGLE*
1	1.4950	0.6255	1.4071	2.5330	-0.4125	53.5838
2	-2.0542	-0.8595	-1.6523	0.3001	-3.2138	-35.0625
3	-1.8478	-1.4688	-1.5697	-0.0772	-3.2394	-41.5581
4	-1.9416	-1.5081	-1.7730	0.0614	-3.5111	-41.5144
5	-2.4249	-1.0147	-1.7955	0.2092	-3.6488	-34.2799
6	2.2602	1.3520	1.7601	3.6239	-0.0116	52.2334
7	-2.3429	-1.3366	-1.8996	0.0941	-3.8236	-37.9356
8	-2.0558	-1.7809	-1.8776	-0.0358	-3.8010	-42.9064
9	-2.2681	-1.8697	-2.1199	0.0603	-4.1981	-42.3163
10	-2.6271	-1.0993	-1.8668	0.1538	-3.8803	-33.8725
11	-2.5275	-1.2598	-1.8543	0.0660	-3.8533	-35.5645
12	-2.5766	-1.2804	-1.9837	0.1584	-4.0154	-35.9534
13	-2.4310	-1.5972	-1.9486	-0.0214	-4.0069	-38.9618
14	-2.5398	-1.6427	-2.1940	0.1482	-4.3306	-39.2231
15	-2.3606	-2.0909	-2.1389	-0.0827	-4.3689	-43.1963
16	-2.5443	-2.1678	-2.4898	0.1409	-4.8530	-42.8381
17	-2.6515	-1.1095	-1.8889	0.1597	-3.9207	-33.8981
18	-2.6590	-1.1755	-1.8739	0.0981	-3.9326	-34.2019
19	-2.6162	-1.1575	-2.0286	0.2689	-4.0426	-35.1128
20	-2.6450	-1.4437	-1.9641	0.0095	-4.0982	-36.4980
21	-2.5932	-1.4221	-2.2270	0.2951	-4.3104	-37.6340
22	-2.6334	-1.8664	-2.1277	-0.0879	-4.4119	-39.8916
23	-2.6159	-1.8591	-2.4840	0.2752	-4.7501	-40.6693
24	-2.6456	-2.4099	-2.3650	-0.1598	-4.8957	-43.5734
25	-2.7295	-2.4450	-2.3250	0.2414	-5.4158	-43.5588
26	-2.4994	-1.0459	-1.8812	0.2441	-3.7894	-34.4384
27	-2.6404	-1.0831	-1.8447	0.1406	-3.8641	-33.5571
28	-2.4641	-1.0093	-2.0523	0.4407	-3.9141	-35.2419
29	-2.6812	-1.3128	-1.9456	0.0654	-4.0594	-35.3127
30	-2.4389	-1.2114	-2.2425	0.4998	-4.1501	-37.3471
31	-2.7071	-1.6942	-2.0886	-0.0515	-4.3497	-38.1846
32	-2.4500	-1.5866	-2.4584	0.4777	-4.5143	-40.0199
33	-2.7492	-2.1776	-2.2759	-0.1696	-4.7572	-41.4216
34	-2.5260	-2.0843	-2.7157	0.4195	-5.0298	-42.6751
35	-2.8337	-2.6942	-2.5276	-0.2354	-5.2925	-44.2094
36	-2.7483	-2.6584	-3.0356	0.3326	-5.7393	-44.5761
37	-2.1792	-0.9118	-1.8586	0.4182	-3.5092	-35.5872
38	-2.4669	-0.9680	-1.7881	0.2213	-3.6563	-33.6304
39	-2.1322	-0.8280	-2.0711	0.6912	-3.6515	-36.2614
40	-2.5400	-1.1907	-1.9132	0.1633	-3.8940	-35.2877
41	-2.1055	-1.0089	-2.2573	0.7658	-3.8801	-38.1736
42	-2.5828	-1.5553	-2.0474	0.0419	-4.1799	-37.9572
43	-2.1079	-1.3566	-2.4418	0.7383	-4.2027	-40.6271
44	-2.6292	-2.0148	-2.2000	-0.1006	-4.5433	-41.0251
45	-2.1388	-1.8096	-2.6397	0.6706	-4.6190	-43.2158
46	-2.7050	-2.5120	-2.3796	-0.2269	-4.9901	-43.8387
47	-2.2303	-2.3133	-2.8266	0.5551	-5.0988	-45.4209
48	-2.8395	-2.8765	-2.5863	-0.2717	-5.4444	-45.2048
49	-2.5263	-2.7455	-3.0015	0.3676	-5.6394	-46.0453
50	-1.6927	-0.7083	-1.8318	0.6962	-3.0973	-37.4797
51	-2.1405	-0.8196	-1.7172	0.3598	-3.3199	-34.4808
52	-1.6252	-0.6039	-2.0968	1.0435	-3.2726	-38.1567
53	-2.2327	-1.0680	-1.8771	0.3150	-3.6157	-36.3825
54	-1.6188	-0.8111	-2.2727	1.0934	-3.5233	-39.9625
55	-2.2800	-1.4259	-2.0111	0.2030	-3.9089	-39.0062
56	-1.6494	-1.1621	-2.4332	1.0396	-3.8511	-42.1407
57	-2.3223	-1.8689	-2.1504	0.0667	-4.2579	-41.9915
58	-1.6842	-1.6019	-2.6053	0.9626	-4.2487	-44.5480
59	-2.3751	-2.3744	-2.3053	-0.0695	-4.6801	-44.9555

62	-1.7717	-2.5471	-2.7343	0.8024	-4.9209	-49.0389
63	-2.5519	-2.8066	-2.5211	-0.1550	-5.2036	-46.4459
64	-2.3353	-2.7160	-2.5571	0.0385	-5.0898	-47.1289
65	-1.0101	-0.4227	-1.8101	1.1174	-2.5501	-40.3916
66	-1.6615	-0.6336	-1.6333	0.5647	-2.8597	-36.2662
67	-0.9232	-0.3246	-2.1371	1.5340	-2.7819	-41.0139
68	-1.7726	-0.9563	-1.8335	0.5139	-3.2428	-38.7248
69	-0.9772	-0.6234	-2.2701	1.4767	-3.0773	-42.7726
70	-1.8252	-1.3046	-1.9566	0.4090	-3.5388	-41.2107
71	-1.0333	-0.9942	-2.3982	1.3599	-3.4373	-44.4677
72	-1.8840	-1.7227	-2.0847	0.2829	-3.8896	-43.8922
73	-1.1719	-1.4247	-2.5649	1.2697	-3.8664	-46.4106
74	-1.9551	-2.2494	-2.2353	0.1379	-4.3424	-46.8831
75	-1.3163	-1.9821	-2.6634	1.0349	-4.3333	-48.5623
76	-2.0239	-2.7479	-2.3613	0.0030	-4.7748	-49.3581
77	-1.5875	-2.5653	-2.7085	0.6758	-4.8287	-50.1160
78	-2.1279	-3.3990	-2.4268	-0.2548	-5.2721	-52.3375
79	-0.7398	-2.8182	-2.0776	0.5440	-4.1020	-58.2864
80	-2.1375	-2.2435	-1.9089	-0.2808	-4.1002	-45.7947
81	-2.0882	-2.2228	-2.5639	0.4093	-4.7203	-45.7521
82	0.0	0.0	-1.8043	1.8043	-1.8043	-45.0000
83	-1.0018	-0.4028	-1.5163	0.8433	-2.2479	-39.4138
84	0.0083	0.0199	-2.1873	2.2013	-2.1732	-44.9244
85	-1.1554	-0.8795	-1.7643	0.7523	-2.7871	-42.7645
86	-0.2009	-0.4801	-2.2134	1.8773	-2.5583	-46.8043
87	-1.2272	-1.2210	-1.8511	0.6270	-3.0752	-44.9521
88	-0.3589	-0.8577	-2.2921	1.6974	-2.9140	-48.1049
89	-1.3325	-1.5898	-1.9425	0.4356	-3.4079	-46.8942
90	-0.5236	-1.2513	-2.4666	1.6058	-3.3807	-49.1956
91	-1.4844	-2.1713	-2.0810	0.2813	-3.9370	-49.6861
92	-0.7864	-1.8792	-2.5172	1.2430	-3.9086	-51.1240
93	-1.6404	-2.7565	-2.1622	0.0347	-4.4316	-52.2362
94	-1.0501	-2.5096	-2.4501	0.7767	-4.3363	-53.2926
95	-1.8263	-3.1359	-2.1625	-0.2215	-4.7407	-53.4227
96	-1.2031	-2.8751	-1.7947	-0.0593	-4.0190	-57.4839
97	-0.9515	-3.3241	-1.7542	-0.0201	-4.2555	-62.0342
98	-0.5200	-1.2427	-2.2693	1.4166	-3.1793	-49.5235
99	-2.3215	-2.7806	-2.4097	-0.1304	-4.9717	-47.7204
100	-0.9177	-2.1931	-2.0000	0.5438	-3.6546	-53.8429

*Clockwise angle from vertical of line of action
of maximum stress for element N.

LIST OF REFERENCES CITED

- (1) Ural, Oktay. Finite Element Method. New York: Intext Education Publishers, 1975.
- (2) Zienkiewicz, O.C. The Finite Element Method in Engineering Science. London: McGraw-Hill Publishing Company Limited, 1971.
- (3) Salmon, C.G. Bracket Plates Without Diagonal Edge Stiffeners. Ann Arbor: University Microfilms International, 1961.
- (4) Buettner, Donald R. and O'Sheridan, Thomas C. Master's Thesis: Laboratory Investigations of Triangular Bracket Plates Without Diagonal Edge Stiffeners. University of Wisconsin, Madison, 1961.
- (5) Timoshenko, S.P. Theory of Elastic Stability. New York: McGraw-Hill Book Co., 1936.
- (6) Ritz, W. Über eine neue Methode zur Lösung gewisser Variations--Probleme der Mathematischen Physik. : Zeitschrift für Reine und Angewendte Mathematik, 1909.
- (7) American Institute of Steel Construction, Inc. Manual of Steel Construction. New York: American Institute of Steel Construction Publisher, 1973.
- (8) Blodgett, Omer W. Design of Welded Structures. New York: The James F. Lincoln Arc Welding Foundation, 1966.